

Data-intrinsic approximation in metric spaces

J. Dölz*[†] and M. Multerer[‡]

Abstract

Analysis and processing of data is a vital part of our modern society and requires vast amounts of computational resources. To reduce the computational burden, compressing and approximating data has become a central topic. We consider the approximation of labeled data samples, mathematically described as site-to-value maps between finite metric spaces. Within this setting, we identify the discrete modulus of continuity as an effective data-intrinsic quantity to measure regularity of site-to-value maps without imposing further structural assumptions. We investigate the consistency of the discrete modulus of continuity in the infinite data limit and propose an algorithm for its efficient computation. Building on these results, we present a sample based approximation theory for labeled data. For data subject to statistical uncertainty we consider multilevel approximation spaces and a variant of the multilevel Monte Carlo method to compute statistical quantities of interest. Our considerations connect approximation theory for labeled data in metric spaces to the covering problem for (random) balls on the one hand and the efficient evaluation of the discrete modulus of continuity to combinatorial optimization on the other hand. We provide extensive numerical studies to illustrate the feasibility of the approach and to validate our theoretical results.

Keywords: data-centric approximation, discrete modulus of continuity, approximation theory

MSC2020: 41A25, 62H11, 65J05

1 Introduction

1.1 Motivation

The analysis and processing of social network data, text data, audio files, photos, and videos, as well as scientific data such as measurements and simulations, have become vital to our modern society. It is estimated that in the year 2023 the world created, captured, copied, and consumed around 123 zettabytes, that is, $123 \cdot 10^{21}$ bytes of data. This number is expected to rise to almost 400 zettabytes by 2028, compare [47]. Processing and storing these data requires immense computational resources. Therefore, the compression and approximation of data is imperative to mitigate the computational burden. In this article, we consider *labeled data*, such as time series, images or videos, where a label or value is assigned to each instance of the data. To mathematically formalize such data, we introduce *site-to-value maps* defined on a finite set X_N of N *data sites* taking *data values* in a set Y_N . Hence, approximating labeled data amounts to the approximation of the site-to-value maps.

The approximation of site-to-value maps is understood as inferring simpler representations of site-to-value maps without having to necessarily process all data instances. Computational efficiency and error estimates may then be derived from additional knowledge. The latter is closely tied to the model selection problem, which makes the pivotal assumption that the site-to-value map is the discretization of some unknown function that belongs to a certain class to derive approximation rates. The applied approximation scheme is then dependent on this presumed class. Typically, the approximation error then depends on the particular choice of the function class, introducing potential bias and uncertainty in the approximation. In a data-centric world, where data themselves are the most relevant source of information, making additional assumptions about their behavior for the purpose of approximation may be unwarranted. It is more natural to develop an approximation theory and algorithms that only operate on the available data. In the present article, we propose such an approximation theory.

*Corresponding author

[†]Institute for Numerical Simulation, University of Bonn, Germany. doelz@ins.uni-bonn.de

[‡]Dalle Molle Institute for Artificial Intelligence, USI Lugano, Switzerland. michael.multerer@usi.ch

1.2 Literature review

There exists an abundance of model-centric approximation schemes for site-to-value, especially in the Euclidean setting. The underlying principle is to represent the site-to-value map by a dictionary of functions, such as polynomials, splines or wavelets, possibly discarding coefficients with small or vanishing effect on the overall representation, see [14, 15, 19, 42, 50] and the references therein. For scattered data sites, approximation in reproducing kernel Hilbert spaces is a standard approach, see, for example, [51]. Under an additional Gaussian process model assumption, even uncertainty quantification is available, see [44]. These approaches may be combined with subsampling, such as the Nyström approximation, see [52], or greedy strategies, see [45], to achieve computational efficiency. For the non-Euclidean setting, Euclidean embeddings of preimage and image spaces can be used to approximate the induced map with techniques for Euclidean spaces. Such embeddings can be realized in a classical analytical fashion or using kernel-induced feature maps, auto encoders and other dimensionality reducing techniques, see [7] and the references therein. In this regard, neural networks have gained particular interest, see, for example, [26, 32, 41].

For general data sites, data-centric approximation schemes become relevant. Examples of such approaches are random forests, see [8], Haar-wavelets on trees, see [24], or diffusion wavelets on graphs, see [12]. More recently, samplets, which form a multiresolution analysis of localized, discrete signed measures, have been introduced, see [29] for a survey and [22] for a construction on graphs.

Data-centric, wavelet like bases particularly allow to measure smoothness of data. In [24], Hölder spaces of discrete data have been introduced. This notion has been generalized by means of microlocal spaces, see [34], on discrete data in [2]. The idea of approximating moduli of smoothness, see, for example, [18], is considered in [16] for certain univariate point distributions, while dyadic meshes grids are considered in [17]. In these approaches, smoothness is measured in terms of available derivatives, or more generally, in terms of bounds on Hölder exponents. Even so, in certain applications, this may be a too crude measure for the particular data instance. Therefore, we pursue an approach based on the *modulus of continuity* and its discretization, respectively. The modulus of continuity is attributed to Lebesgue, see [39, 48], and provides regularity information for any continuous function defined between metric spaces, without imposing additional assumptions.

1.3 The approach taken

The first straightforward observation we make and exploit is that site-to-value maps are trivially continuous functions, if we equip the domain X_N and the range Y_N with the structure of compact metric spaces. The second observation is that every continuous function on a compact metric space exhibits a (optimal) modulus of continuity. As a rule of thumb, the faster the decay of the modulus of continuity towards zero, the more regular the function. As a consequence, the modulus of continuity has become a valuable tool in approximation theory and analysis, see [5, 15, 31, 33].

For the specific setting of site-to-value maps $f_N: X_N \rightarrow Y_N$, the (discrete) modulus of continuity reads

$$\omega(Y_N, t) := \max_{\substack{\mathbf{x}, \mathbf{x}' \in X_N : \\ d_{X_N}(\mathbf{x}, \mathbf{x}') \leq t}} d_{Y_N}(f_N(\mathbf{x}), f_N(\mathbf{x}')),$$

and amounts to a measure of regularity of site-to-value maps, see Figure 1 for two illustrating examples. As a maximum over a set of finite cardinality, the discrete modulus of continuity is, in principle, computationally accessible from the data. This leads us to the following questions.

- (Q1) When is the modulus of continuity of site-to-value maps consistent in the infinite data limit?
- (Q2) How can we efficiently compute or estimate the modulus of continuity from data?
- (Q3) How can we exploit the data-intrinsic regularity provided by the modulus of continuity to construct efficient approximation schemes for site-to-value maps?

By providing answers and follow up questions to (Q1) to (Q3), the aim of this article is to derive data-intrinsic approximation schemes and rates which only exploit the data-intrinsic regularity provided by the discrete modulus of continuity $\omega(Y_N, t)$.

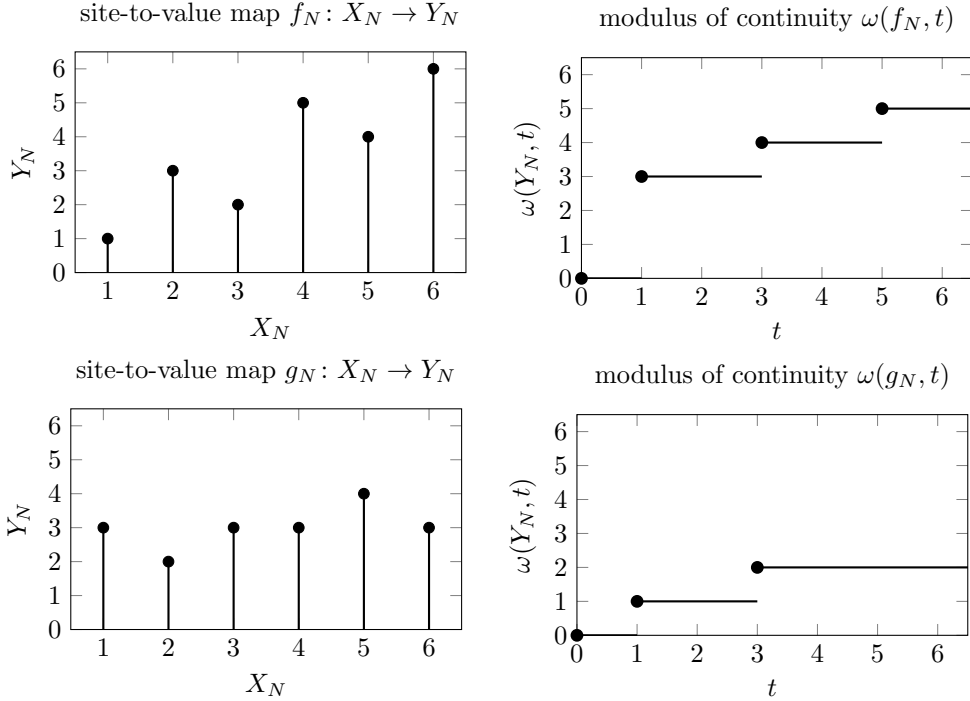


Figure 1: Illustration of two continuous functions $f_N, g_N: \{1, \dots, 6\} \rightarrow \mathbb{N}$ (left) and their corresponding discrete, optimal, right-continuous moduli of continuity as a measure of their smoothness (right).

1.4 Contributions

Guided by the questions (Q1) to (Q3), the contributions of this article to the approximation of site-to-value maps $f_N: X_N \rightarrow Y_N$ between finite metric spaces are as follows.

- (C1) For both, deterministically chosen and empirical data sites, we provide point-wise and L^p approximation rates and consistency analyses of the modulus of continuity in the infinite data limit. To this end, we connect the question of approximation to the (random) set cover problem of (random) balls and to covering numbers. This addresses (Q1).
- (C2) We provide an algorithm for the efficient approximation of the modulus of continuity. To do this, we establish connections to nearest neighbor searches and combinatorial integer optimization. This addresses (Q2).
- (C3) We establish an interpolation-based approximation theory of piecewise constant functions for deterministic and random site-to-value maps. To achieve the latter, we construct multilevel approximation spaces on labeled data and provide a natural extension of the multilevel Monte Carlo method to labeled data in metric spaces. This addresses (Q3).

We complement these contributions with non-trivial numerical examples, illustrating the feasibility of the approach and the validity of our theoretical results.

1.5 Outline

The remainder of this article is structured as follows. In Section 2, we introduce the discrete modulus of continuity and transfer well known results from literature to the discrete setting. Section 3 studies the consistency of the discrete modulus of continuity for deterministic data sites. The consistency of the discrete modulus of continuity for empirical data sites is addressed in Section 4 by assuming that data sites are independent samples of a given probability distribution. In Section 5, we address the efficient computation of the discrete modulus of continuity, avoiding the naive quadratic cost in terms of the number of data sites. Section 6 derives approximation results for the piecewise constant approximation of site-to-value maps. As a relevant application of the present framework, we consider the multilevel Monte Carlo method for the computation of first

and second order statistics of high-dimensional random vectors in Section 7. Extensive numerical results are presented in Section 8 and concluding remarks are stated in Section 9.

2 Moduli of continuity

Let $(\mathcal{X}, d_{\mathcal{X}})$ and $(\mathcal{Y}, d_{\mathcal{Y}})$ be metric spaces and assume that \mathcal{X} be compact with diameter

$$T_{\mathcal{X}} := \text{diam}(\mathcal{X}) < \infty.$$

Given a set of *data points*

$$\{(\mathbf{x}_1, \mathbf{y}_1), \dots, (\mathbf{x}_N, \mathbf{y}_N)\} \subset \mathcal{X} \times \mathcal{Y} \quad (1)$$

comprised of *data sites* $X_N = \{\mathbf{x}_1, \dots, \mathbf{x}_N\}$ and *data values* $Y_N = \{\mathbf{y}_1, \dots, \mathbf{y}_N\}$, we aim at deriving a notion of smoothness for the *site-to-value map*

$$f_N: X_N \rightarrow Y_N, \quad \mathbf{x}_i \mapsto \mathbf{y}_i. \quad (2)$$

We introduce the following quantities.

Definition 2.1. *The fill distance is defined as*

$$h_{X_N} := \sup_{\mathbf{x} \in \mathcal{X}} \min_{\mathbf{x}_i \in X} d_{\mathcal{X}}(\mathbf{x}, \mathbf{x}_i), \quad (3)$$

whereas the separation distance is given by

$$q_{X_N} := \min_{i \neq j} d_{i,j} \quad (4)$$

with the distance matrix $\mathbf{D} := [d_{i,j}]_{i,j=1}^N$, $d_{i,j} := d_{\mathcal{X}}(\mathbf{x}_i, \mathbf{x}_j)$.

The set X_N is quasi-uniform, if there exists a constant $c > 0$ such that

$$\frac{1}{c} q_{X_N} \leq h_{X_N} \leq c q_{X_N}. \quad (5)$$

To define a *discrete modulus of continuity*, we first recall the classical definition of the *modulus of continuity*, see, for example, [5, 15].

Definition 2.2. *We say that the modulus of continuity is continuous if it is continuous with respect to the canonical topology of $[0, \infty] = \mathbb{R}_{\geq 0} \cup \{\infty\}$.*

For a monotonically increasing function $\rho: [0, \infty] \rightarrow [0, \infty]$ we further introduce the semi-norm

$$|f|_{\rho} := \sup_{t > 0} \rho(t)^{-1} \omega(f, t)$$

and say that f is of class ρ if $|f|_{\rho} < \infty$.

Remark 2.3. 1. The most natural classes ρ are the ones generated by functions which are moduli of continuity themselves.

2. The modulus of continuity of a function f of class ρ satisfies

$$\omega(f, t) \leq \rho(t) |f|_{\rho}.$$

3. The seminorm in the previous definition allows us to introduce function classes in terms of the modulus of continuity. For $\rho(t) = t^{\alpha}$ we obtain the well known $|\cdot|_{\text{Lip}(\alpha)}$ -seminorm.

We collect the basic properties of the modulus of continuity in the following lemma, see, for example, [15].

Lemma 2.4 (Properties of the modulus of continuity). *Let $f: \mathcal{X} \rightarrow \mathcal{Y}$ be uniformly continuous. Then, the modulus of continuity*

1. is continuous at 0 and $\omega(f, t) \rightarrow \omega(f, 0) = 0$ for $t \rightarrow 0$.
2. is non-negative, continuous and non-decreasing for $t > 0$.

Remark 2.5.

1. Since \mathcal{X} is compact, we note that any continuous function $f: \mathcal{X} \rightarrow \mathcal{Y}$ is also uniformly continuous, that is, for each $\varepsilon > 0$ there exists $\delta > 0$ such that for all $\mathbf{x}, \mathbf{x}' \in \mathcal{X}$ with $d_{\mathcal{X}}(\mathbf{x}, \mathbf{x}') < \delta$ there holds $d_{\mathcal{Y}}(f(\mathbf{x}), f(\mathbf{x}')) < \varepsilon$.
2. In the literature, the modulus of continuity from Definition 2.2 is often referred to as the optimal modulus of continuity.
3. Vice versa, any function which satisfies the assertions of Lemma 2.4 and is a majorant to the (optimal) modulus of continuity is considered as a modulus of continuity. Throughout this article we do not rely on this distinction and always refer to the optimal modulus of continuity from Definition 2.2, whenever we refer to the modulus of continuity.

Every site-to-value map $f_N: X_N \rightarrow Y_N \subset \mathcal{Y}$, see (2), is uniformly continuous, which is immediate by choosing $0 < \delta < q_X$, compare the first item of Remark 2.5. Moreover, $(X_N, d_{\mathcal{X}})$ is a metric space by restricting the metric of \mathcal{X} to X_N . This stipulates the definition of the *discrete modulus of continuity* for $f: \mathcal{X} \rightarrow \mathcal{Y}$ according to

$$\omega_N(f, t) = \max_{\substack{\mathbf{x}_i, \mathbf{x}_j \in X_N: \\ d_{i,j} \leq t}} d_{\mathcal{Y}}(f(\mathbf{x}_i), f(\mathbf{x}_j)). \quad (6)$$

Remark 2.6.

1. The properties from Lemma 2.4 directly carry over to $\omega_N(f, t)$.
2. The definition (6) does not require the knowledge of a function f defined on all of \mathcal{X} .
3. Vice versa, one can always find a function $f: \mathcal{X} \rightarrow \mathcal{Y}$ with $f(\mathbf{x}_i) = \mathbf{y}_i$ for $i = 1, \dots, N$. Therefore, it is possible to define the discrete modulus of continuity exclusively using the set of data points. To emphasize this fact, we may also write

$$\omega_N(Y_N, t) := \max_{\substack{\mathbf{y}_i, \mathbf{y}_j \in Y_N: \\ d_{i,j} \leq t}} d_{\mathcal{Y}}(\mathbf{y}_i, \mathbf{y}_j). \quad (7)$$

4. We will later adopt the perspective that \mathcal{X} is a finite set of data sites and X_N a subset thereof. In this case the continuous modulus of continuity from Definition 2.2 and the discrete modulus of continuity from Equation (7) coincide on \mathcal{X} .

We have the following result for the discrete modulus of continuity with respect to the set of data sites.

Lemma 2.7 (Monotonicity of discrete modulus of continuity). *Let $X_N \subset X_{N'}$ for $N' \geq N$. Then there holds*

$$\omega_N(f, t) \leq \omega_{N'}(f, t) \leq \omega(f, t), \quad t \geq 0,$$

for any function $f: \mathcal{X} \rightarrow \mathcal{Y}$.

Proof. Without loss of generality, let $X_{N'} = X_N \cup \{\mathbf{x}_{N+1}, \dots, \mathbf{x}_{N'}\}$. We introduce the index sets

$$I_{N,t} := \{(i, j) \in \{1, \dots, N\}^2 : d_{i,j} \leq t\}$$

and observe $I_{N,t} \subset I_{N',t}$ for any $N' \geq N$ and any $t \geq 0$. Analogously, we define the sets

$$F_{N,t} := \{d_{\mathcal{Y}}(f(\mathbf{x}_i), f(\mathbf{x}_j)) : (i, j) \in I_{N,t}\}, \quad (8)$$

which satisfy $F_{N,t} \subset F_{N',t}$. Therefore, we infer

$$\omega_N(f, t) = \max F_{N,t} \leq \max F_{N',t} = \omega_{N'}(f, t) \quad \text{for any } t \geq 0.$$

The second bound follows in complete analogy. \square

The discrete modulus of continuity gives rise to a discrete version of the $|\cdot|_\rho$ -seminorm. We define

$$|f|_{\rho, N} := \max_{i,j \in \{1, \dots, N\}: i \neq j} \rho(d_{i,j})^{-1} \omega_N(f, d_{i,j}). \quad (9)$$

Again, in complete analogy, if only a site-to-value map $f_N: X_N \rightarrow Y_N$ is known, we set

$$|f_N|_{\rho, N} := \max_{i,j \in \{1, \dots, N\}: i \neq j} \rho(d_{i,j})^{-1} \omega_N(Y_N, d_{i,j}). \quad (10)$$

Lemma 2.8 (Monotonicity of the discrete seminorm). *Let $X_N \subset X_{N'}$ for $N' \geq N$. Then there holds*

$$|f|_{\rho, N} \leq |f|_{\rho, N'} \leq |f|_\rho$$

for any function $f: \mathcal{X} \rightarrow \mathcal{Y}$.

Proof. The assertion is an immediate consequence of Lemma 2.7. \square

3 Consistency for deterministic data sites

In this section, we derive consistency estimates for the discrete modulus of continuity for deterministic data sites that meet specific properties. More precisely, we assume that the site-to-value map $f_N: X_N \rightarrow Y_N$ is the restriction of some function $f: \mathcal{X} \rightarrow \mathcal{Y}$, that is, $f_N = f|_{X_N}$. We derive approximation estimates of the discrete modulus of continuity $\omega_N(Y_N, \cdot) = \omega_N(f, \cdot)$ to the modulus of continuity $\omega(f, \cdot)$ and discuss the consistency behavior for $N \rightarrow \infty$. To this end, we require no further assumptions on \mathcal{X} despite of it being a compact metric space. For example, \mathcal{X} may be a finite but larger set than X_N or a metric space of infinite cardinality in which the data sites are embedded.

3.1 Covering numbers

Definition 3.1. *An ε -net for $(\mathcal{X}, d_{\mathcal{X}})$ is a subset $\mathcal{K} \subset \mathcal{X}$ such that for each $\mathbf{x} \in \mathcal{X}$ there exists $\mathbf{x}' \in \mathcal{K}$ with $\mathbf{x} \in B_\varepsilon(\mathbf{x}') := \{\mathbf{x} \in \mathcal{X} : d_{\mathcal{X}}(\mathbf{x}, \mathbf{x}') \leq \varepsilon\}$. The smallest cardinality of an ε -net for \mathcal{X} is the covering number $\mathcal{N}(\mathcal{X}, \varepsilon)$, that is,*

$$\mathcal{N}(\mathcal{X}, \varepsilon) := \min\{|\mathcal{K}| : \mathcal{K} \text{ is an } \varepsilon\text{-net for } (\mathcal{X}, d_{\mathcal{X}})\}. \quad (11)$$

Remark 3.2. *Sometimes, it is assumed that an ε -net $\mathcal{K} \subset \mathcal{X}$ is also an $\varepsilon/2$ -packing in the sense that $\mathbf{x} \notin B_{\varepsilon/2}(\mathbf{x}')$ for all $\mathbf{x}, \mathbf{x}' \in \mathcal{K}$ with $\mathbf{x} \neq \mathbf{x}'$, see, for example, [6, 11, 38]. In this case, the covering number can be shown to be equivalent to the packing number*

$$\mathcal{P}(\mathcal{X}, \varepsilon) := \max\{|\mathcal{K}| : \mathcal{K} \text{ is an } \varepsilon\text{-packing for } (\mathcal{X}, d_{\mathcal{X}})\}$$

meaning that $\mathcal{P}(\mathcal{X}, \varepsilon) \leq \mathcal{N}(\mathcal{X}, \varepsilon) \leq \mathcal{P}(\mathcal{X}, \varepsilon/2)$, see [36, Theorem 4].

It follows directly from Definition 3.1 that

$$\mathcal{N}(\mathcal{X}, \varepsilon) \geq \mathcal{N}(\mathcal{X}, \varepsilon') \quad (12)$$

for all $0 \leq \varepsilon < \varepsilon'$.

While the covering number is rarely accessible in closed form, upper and lower bounds to it have been the subject of several investigations in the literature. In the following, we give three intuitive examples.

Example 3.3. 1. If $\mathcal{X} \subset \mathbb{R}^d$ is equipped with the Euclidean metric, then it is a standard result that

$$\frac{\lambda(\mathcal{X})}{\lambda(B_r(0))} \leq \mathcal{N}(\mathcal{X}, r) \leq 3^d \frac{\lambda(\mathcal{X})}{\lambda(B_r(0))},$$

where λ is the Lebesgue measure on \mathbb{R}^d .

2. More generally, a metric space \mathcal{X} is Ahlfors n -regular, if there exists a Borel regular measure μ and constants $C \geq 1$, $n > 0$ such that $C^{-1}R^n \leq \mu(B_R(\mathbf{x})) \leq CR^n$ for all $\mathbf{x} \in \mathcal{X}$, $R > 0$, see [31]. By the same arguments as for \mathbb{R}^d , the covering number of an Ahlfors n -regular space satisfies

$$c^{-1}r^{-n} \leq \mathcal{N}(\mathcal{X}, r) \leq cr^{-n}$$

for all $r > 0$ and some constant $c > 0$. Especially, the Euclidean space \mathbb{R}^d is Ahlfors d -regular.

3. The metric space $(\mathcal{X}, d_{\mathcal{X}})$ is (C, s) -homogeneous, if

$$\mathcal{N}(B_R(\mathbf{x}), r) \leq C \left(\frac{R}{r} \right)^s$$

for all $\mathbf{x} \in \mathcal{X}$ and all $0 < r < R < \infty$. The infimum of the set of all s such that $(\mathcal{X}, d_{\mathcal{X}})$ is (C, s) -homogeneous is the Assouad dimension of $(\mathcal{X}, d_{\mathcal{X}})$, see [1]. For a metric space with Assouad dimension s there holds

$$\mathcal{N}(\mathcal{X}, r) \leq cr^{-s}, \quad (13)$$

with a constant $c > 0$ depending on \mathcal{X} . In particular, an Ahlfors n -regular metric space has Assouad dimension n . Finally, we remark that the Assouad dimension of a finite metric space is 0.

An important property of ε -nets is that their covering property is preserved in the image of a given metric.

Lemma 3.4 (Metric maps $\varepsilon/2$ -nets to ε -nets). *Let (\mathcal{X}, d) be a compact metric space, $\varepsilon > 0$, and $X_N = \{\mathbf{x}_1, \dots, \mathbf{x}_N\}$ an $\varepsilon/2$ -net. Let $Z_N \subset \mathcal{Z} \subset [0, \infty]$ be defined as*

$$Z_N = \{d_{\mathcal{X}}(\mathbf{x}, \mathbf{x}') : \mathbf{x}, \mathbf{x}' \in X_N\}, \quad \mathcal{Z} = \{d_{\mathcal{X}}(\mathbf{x}, \mathbf{x}') : \mathbf{x}, \mathbf{x}' \in \mathcal{X}\}. \quad (14)$$

Then Z_N is an ε -net for \mathcal{Z} , that is, there holds

$$\bigcup_{\mathbf{z} \in Z_N} B_{\varepsilon}(\mathbf{z}) = \mathcal{Z}.$$

Proof. We show that for all $t \in \mathcal{Z}$ there is $s \in Z_N$ such that $|t - s| \leq \varepsilon$. Let $t \in \mathcal{Z}$. Hence, there exist $\mathbf{x}, \tilde{\mathbf{x}} \in \mathcal{X}$ such that $t = d_{\mathcal{X}}(\mathbf{x}, \tilde{\mathbf{x}})$. Moreover, since X_N is a $\varepsilon/2$ -net for \mathcal{X} , there further exist $\mathbf{x}_i, \mathbf{x}_j \in X_N$ such that

$$d_{\mathcal{X}}(\mathbf{x}, \mathbf{x}_i) \leq \frac{\varepsilon}{2}, \quad d_{\mathcal{X}}(\mathbf{x}', \mathbf{x}_j) \leq \frac{\varepsilon}{2}.$$

Thus, we have $s = d_{\mathcal{X}}(\mathbf{x}_i, \mathbf{x}_j) \in Z_N$ and it remains to bound $|t - s|$.

First let $t \geq s$. By the triangle inequality, we derive

$$\begin{aligned} t - s &= d_{\mathcal{X}}(\mathbf{x}, \mathbf{x}') - d_{\mathcal{X}}(\mathbf{x}_i, \mathbf{x}_j) \\ &\leq d_{\mathcal{X}}(\mathbf{x}, \mathbf{x}_i) + d_{\mathcal{X}}(\mathbf{x}_i, \mathbf{x}_j) + d_{\mathcal{X}}(\mathbf{x}_j, \mathbf{x}') - d_{\mathcal{X}}(\mathbf{x}_i, \mathbf{x}_j) \\ &= d_{\mathcal{X}}(\mathbf{x}, \mathbf{x}_i) + d_{\mathcal{X}}(\mathbf{x}', \mathbf{x}_j) \\ &\leq \varepsilon. \end{aligned}$$

Now, let $t < s$. Analogously, we infer

$$\begin{aligned} s - t &= d_{\mathcal{X}}(\mathbf{x}_i, \mathbf{x}_j) - d_{\mathcal{X}}(\mathbf{x}, \mathbf{x}') \\ &\leq d_{\mathcal{X}}(\mathbf{x}_i, \mathbf{x}) + d_{\mathcal{X}}(\mathbf{x}, \mathbf{x}') + d_{\mathcal{X}}(\mathbf{x}', \mathbf{x}_j) - d_{\mathcal{X}}(\mathbf{x}, \mathbf{x}') \\ &= d_{\mathcal{X}}(\mathbf{x}, \mathbf{x}_i) + d_{\mathcal{X}}(\mathbf{x}', \mathbf{x}_j) \\ &\leq \varepsilon. \end{aligned}$$

Combining the two estimates proves the assertion. \square

An immediate consequence of this lemma is the following consistency result for continuous moduli of continuity.

Corollary 3.5 (Consistency for continuous moduli of continuity). *Let $f: \mathcal{X} \rightarrow \mathcal{Y}$ have a continuous modulus of continuity. Moreover, let $\{X_N\}_{N \in \mathbb{N}}$ be a sequence of $r_N/2$ -nets with $r_N \rightarrow 0$. Then*

$$\omega(f, t) - \omega_N(f, t) \rightarrow 0 \quad \text{as } N \rightarrow \infty.$$

The convergence is uniform in t .

Proof. Convergence for fixed t follows directly from Lemma 3.4. Moreover, the function f having a modulus of continuity implies continuity of f . Since \mathcal{X} is compact, the function f is even uniformly continuous, which, in turn, implies the uniform convergence in t . \square

We note that even a uniformly continuous function on a compact metric space is not required to have a continuous modulus of continuity if \mathcal{Z} in Lemma 3.4 is a non-convex set. In fact, non-constant site-to-value maps have always discontinuous moduli of continuity, such that a more refined analysis is required. In the following we provide such an analysis.

3.2 Pointwise approximation

The following theorem bounds the approximation error of the discrete modulus of continuity compared to the continuous one at a given point $t > 0$. For $t = 0$, there always holds $\omega(f, 0) = \omega_N(f, 0) = 0$, see also Lemma 2.4.

Theorem 3.6 (Covering diameter $r < t$ implies error bound at t). *Let $f: \mathcal{X} \rightarrow \mathcal{Y}$ be continuous. Let $t > 0$ be fixed and let $X_N = \{\mathbf{x}_1, \dots, \mathbf{x}_N\}$, $N \geq \mathcal{N}(\mathcal{X}, r/2)$, be an $r/2$ -net for $0 < r \leq t$, that is,*

$$\bigcup_{n=1}^N B_{r/2}(\mathbf{x}_n) = \mathcal{X}. \quad (15)$$

Then, there holds

$$0 \leq \omega(f, t) - \omega_N(f, t) \leq \omega(f, t) - \omega(f, t - r) + 2\omega(f, r).$$

Proof. From Lemma 2.7, we have

$$0 \leq \omega(f, t) - \omega_N(f, t) = \omega(f, t) - \omega(f, t - r) + \underbrace{\omega(f, t - r) - \omega_N(f, t)}_{=(\spadesuit)}. \quad (16)$$

To prove the assertion, we need to estimate (\spadesuit) . The definition of the modulus of continuity implies

$$(\spadesuit) = \sup_{\substack{\mathbf{x}, \mathbf{x}' \in \mathcal{X} \\ d_{\mathcal{X}}(\mathbf{x}, \mathbf{x}') \leq t - r}} d_{\mathcal{Y}}(f(\mathbf{x}), f(\mathbf{x}')) - \max_{\substack{\tilde{\mathbf{x}}_N, \tilde{\mathbf{x}}'_N \in X_N \\ d_{\mathcal{X}}(\tilde{\mathbf{x}}_N, \tilde{\mathbf{x}}'_N) \leq t}} d_{\mathcal{Y}}(f(\tilde{\mathbf{x}}_N), f(\tilde{\mathbf{x}}'_N)).$$

To allow for a comparison between supremum and maximum, observe that Equation (15) implies that for every $\mathbf{x}, \mathbf{x}' \in \mathcal{X}$ there exist $\mathbf{x}_N, \mathbf{x}'_N \in X_N$ such that

$$d_{\mathcal{X}}(\mathbf{x}, \mathbf{x}_N) \leq \frac{r}{2}, \quad d_{\mathcal{X}}(\mathbf{x}', \mathbf{x}'_N) \leq \frac{r}{2}. \quad (17)$$

As a consequence, for given $\mathbf{x}, \mathbf{x}' \in \mathcal{X}$ with $d_{\mathcal{X}}(\mathbf{x}, \mathbf{x}') \leq t - r$, the problem

$$(\mathbf{x}_N, \mathbf{x}'_N) \in \operatorname{argmin}_{\substack{d_{\mathcal{X}}(\mathbf{x}, \tilde{\mathbf{x}}_N) \leq \frac{r}{2} \\ d_{\mathcal{X}}(\mathbf{x}', \tilde{\mathbf{x}}'_N) \leq \frac{r}{2} \\ d_{\mathcal{X}}(\tilde{\mathbf{x}}_N, \tilde{\mathbf{x}}'_N) \leq t}} (d_{\mathcal{X}}(\mathbf{x}, \tilde{\mathbf{x}}_N) + d_{\mathcal{X}}(\mathbf{x}', \tilde{\mathbf{x}}'_N)) \quad (18)$$

always exhibits a solution. The situation is illustrated in Figure 2. To keep the notation light we suppress the dependence of $(\mathbf{x}_N, \mathbf{x}'_N)$ on $(\mathbf{x}, \mathbf{x}')$.

Now, by observing that the triangle inequality implies the bound

$$d_{\mathcal{Y}}(f(\mathbf{x}), f(\mathbf{x}')) - d_{\mathcal{Y}}(f(\mathbf{x}), f(\mathbf{x}_N)) - d_{\mathcal{Y}}(f(\mathbf{x}'), f(\mathbf{x}'_N)) \leq d_{\mathcal{Y}}(f(\mathbf{x}_N), f(\mathbf{x}'_N))$$

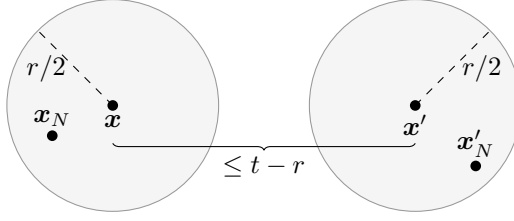


Figure 2: Visualization of the situation in (18).

and that there holds

$$d_{\mathcal{Y}}(f(\mathbf{x}_N), f(\mathbf{x}'_N)) \leq \max_{\substack{\tilde{\mathbf{x}}_N, \tilde{\mathbf{x}}'_N \in X_N \\ d_{\mathcal{X}}(\tilde{\mathbf{x}}_N, \tilde{\mathbf{x}}'_N) \leq t}} d_{\mathcal{Y}}(f(\tilde{\mathbf{x}}_N), f(\tilde{\mathbf{x}}'_N)),$$

we obtain that

$$\begin{aligned} (\spadesuit) &= \sup_{\substack{\mathbf{x}, \mathbf{x}' \in \mathcal{X} \\ d_{\mathcal{X}}(\mathbf{x}, \mathbf{x}') \leq t - r}} d_{\mathcal{Y}}(f(\mathbf{x}), f(\mathbf{x}')) - \max_{\substack{\tilde{\mathbf{x}}_N, \tilde{\mathbf{x}}'_N \in X_N \\ d_{\mathcal{X}}(\tilde{\mathbf{x}}_N, \tilde{\mathbf{x}}'_N) \leq t}} d_{\mathcal{Y}}(f(\tilde{\mathbf{x}}_N), f(\tilde{\mathbf{x}}'_N)) \\ &\leq \sup_{\substack{\mathbf{x}, \mathbf{x}' \in \mathcal{X} \\ d_{\mathcal{X}}(\mathbf{x}, \mathbf{x}') \leq t - r}} \left(d_{\mathcal{Y}}(f(\mathbf{x}), f(\mathbf{x}')) - d_{\mathcal{Y}}(f(\mathbf{x}_N), f(\mathbf{x}'_N)) \right) \\ &\leq \sup_{\substack{\mathbf{x}, \mathbf{x}' \in \mathcal{X} \\ d_{\mathcal{X}}(\mathbf{x}, \mathbf{x}') \leq t - r}} \left(d_{\mathcal{Y}}(f(\mathbf{x}), f(\mathbf{x}')) \right. \\ &\quad \left. - \left(d_{\mathcal{Y}}(f(\mathbf{x}), f(\mathbf{x}')) - d_{\mathcal{Y}}(f(\mathbf{x}), f(\mathbf{x}_N)) - d_{\mathcal{Y}}(f(\mathbf{x}'), f(\mathbf{x}'_N)) \right) \right) \\ &= \sup_{\substack{\mathbf{x}, \mathbf{x}' \in \mathcal{X} \\ d_{\mathcal{X}}(\mathbf{x}, \mathbf{x}') \leq t - r}} \left(d_{\mathcal{Y}}(f(\mathbf{x}), f(\mathbf{x}_N)) + d_{\mathcal{Y}}(f(\mathbf{x}'), f(\mathbf{x}'_N)) \right) \\ &\leq \sup_{\substack{\mathbf{x}, \mathbf{x}' \in \mathcal{X} \\ d_{\mathcal{X}}(\mathbf{x}, \mathbf{x}') \leq t - r}} \left(\omega(f, d_{\mathcal{X}}(\mathbf{x}, \mathbf{x}_N)) + \omega(f, d_{\mathcal{X}}(\mathbf{x}', \mathbf{x}'_N)) \right) \\ &\leq 2\omega(f, r). \end{aligned}$$

Herein, we used the monotonicity of the modulus of continuity in the last inequality. The assertion follows with Equation (16). \square

We note that the theorem recovers Corollary 3.5 if the modulus of continuity is continuous due to $\omega(f, 0) = 0$, see Lemma 2.4. We also note that moduli of continuity having a jump in the left vicinity of t cannot be well approximated. This is to be expected, as discontinuous functions cannot be well approximated by piecewise constant functions, in general, and the discrete modulus of continuity is indeed piecewise constant.

We have the following corollary.

Corollary 3.7 (Best N -term approximation rate at t). *Let $f: \mathcal{X} \rightarrow \mathcal{Y}$ be continuous and let $t > 0$ and $N \in \mathbb{N}$ be fixed. Further, set*

$$r(N, t) := \min \{0 \leq r \leq t: \mathcal{N}(\mathcal{X}, r) \leq N\}.$$

Then, there exists a set $X_N = \{\mathbf{x}_1, \dots, \mathbf{x}_N\}$ such that

$$0 \leq \omega(f, t) - \omega_N(f, t) \leq \omega(f, t) - \omega(f, t - r(N, t)) + 2\omega(f, r(N, t)).$$

Remark 3.8. *The case $r(N, t) = 0$ in Corollary 3.7 implies $|\mathcal{X}| \leq N$. Thus, as $\omega(f, 0) = 0$, and as stated by the corollary, we can choose N samples such that the discrete modulus of continuity coincides with the continuous modulus of continuity.*

3.3 Approximation and consistency on intervals

While the previous results are concerned with the pointwise consistency of the modulus of continuity with respect to t , the following results inspect the consistency with respect to bounded intervals $t \in [a, b]$ in $L^p(a, b)$ with $[a, b] \subset [0, T_{\mathcal{X}}]$.

Theorem 3.9 (Covering diameter $0 < r \leq a$ implies error bound in $L^p(a, b)$). *Let $f: \mathcal{X} \rightarrow \mathcal{Y}$ be continuous and consider $[a, b] \subset (0, T_{\mathcal{X}}]$. Moreover, let $N_r \geq \mathcal{N}(\mathcal{X}, r/2)$, $0 < r \leq a$, and let $X_{N_r} = \{x_1, \dots, x_{N_r}\}$ be an $r/2$ -net. Then, there holds*

$$\|\omega(f, \cdot) - \omega_{N_r}(f, \cdot)\|_{L^p(a, b)} \leq \begin{cases} 2^{\frac{p-1}{p}} \|\omega(f, \cdot) - \omega(f, \cdot - r)\|_{L^p(a, b)} + 2(b-a)^{1/p} \omega(f, r), & p \in [1, \infty), \\ \|\omega(f, \cdot) - \omega(f, \cdot - r)\|_{L^\infty(a, b)} + 2\omega(f, r), & p = \infty. \end{cases}$$

Proof. We first consider the case $p \in [1, \infty)$. Since $t \mapsto t^p$ is convex for $t \geq 0$, there holds

$$\left(\frac{A+B}{2}\right)^p \leq \frac{A^p + B^p}{2}$$

and thus

$$(A+B)^p \leq 2^{p-1}(A^p + B^p)$$

for any $A, B \geq 0$. Next, observing that $A = \omega(f, a) - \omega(f, a-r)$ and $B = 2\omega(f, r)$ are non-negative, see Lemma 2.4, we obtain with Theorem 3.6 that

$$\begin{aligned} \|\omega(f, \cdot) - \omega_{N_r}(f, \cdot)\|_{L^p(a, b)}^p &\leq \int_a^b |\omega(f, t) - \omega(f, t-r) + 2\omega(f, r)|^p dt \\ &\leq 2^{p-1} \int_a^b |\omega(f, t) - \omega(f, t-r)|^p dt + 2^p \int_a^b |\omega(f, r)|^p dt \\ &= 2^{p-1} \|\omega(f, t) - \omega(f, t-r)\|_{L^p(a, b)}^p + 2^p (b-a) \omega(f, r)^p. \end{aligned}$$

Concavity of $t \mapsto t^{1/p}$ yields the assertion for $p \in [1, \infty)$. The assertion for $p = \infty$ follows from Theorem 3.6 and the triangle inequality. \square

A consequence similar to Corollary 3.7 can be stated, which yields the same insights as Remark 3.8. Moreover, close inspection of Theorem 3.9 shows that the requirements on N can be too restrictive if the interval approaches zero, that is, when $a \rightarrow 0$. This is due to the potential growth of the covering number $\mathcal{N}(\mathcal{X}, r)$ when $0 < r \leq a \rightarrow 0$. This issue can be fixed as follows.

Corollary 3.10 (Approximation in $L^p(0, b)$). *Let $f: \mathcal{X} \rightarrow \mathcal{Y}$ be continuous and let $\alpha \in (0, b]$, $b \leq T_{\mathcal{X}}$, such that $N \geq \mathcal{N}(\mathcal{X}, \alpha/2)$. Then, there holds*

$$\begin{aligned} \|\omega(f, \cdot) - \omega_{N_r}(f, \cdot)\|_{L^p(0, b)} &\leq \\ &\leq \begin{cases} \alpha^{1/p} \omega(f, \alpha) + 2^{(p-1)/p} \|\omega(f, \cdot) - \omega(f, \cdot - \alpha)\|_{L^p(\alpha, b)} + 2(b-\alpha)^{1/p} \omega(f, \alpha), & p \in [1, \infty), \\ \omega(f, \alpha) + \|\omega(f, \cdot) - \omega(f, \cdot - \alpha)\|_{L^\infty(\alpha, b)} + 2\omega(f, \alpha), & p = \infty. \end{cases} \end{aligned}$$

Proof. The assertion then follows from

$$\|\omega(f, \cdot) - \omega_N(f, \cdot)\|_{L^p(0, b)} \leq \|\omega(f, \cdot) - \omega_N(f, \cdot)\|_{L^p(0, \alpha)} + \|\omega(f, \cdot) - \omega_N(f, \cdot)\|_{L^p(\alpha, b)}.$$

The first term can be bounded by exploiting the non-negativity, see Lemma 2.4, and monotonicity, see Lemma 2.7, of the discrete modulus of continuity with respect to N according to

$$\|\omega(f, \cdot) - \omega_N(f, \cdot)\|_{L^p(0, \alpha)} \leq \|\omega(f, \cdot)\|_{L^p(0, \alpha)} \leq \begin{cases} \alpha^{1/p} \omega(f, \alpha), & p \in [1, \infty), \\ \omega(f, \alpha), & p = \infty. \end{cases}$$

The second term is bounded by Theorem 3.9. This yields the assertion. \square

The combination of the previous results allow us to prove consistency in $L^p(a, b)$ with $[a, b] \subset [0, T_{\mathcal{X}}]$.

Corollary 3.11 (Consistency in $L^p(a, b)$). *Let $f: \mathcal{X} \rightarrow \mathcal{Y}$ be continuous and let $[a, b] \subset [0, T_{\mathcal{X}}]$. Further let $\{X_{N_k}\}_{k \in \mathbb{N}}$ be a sequence of $r_k/2$ -nets with $r_k \rightarrow 0$ as $k \rightarrow \infty$. Then, there holds*

$$\|\omega(f, \cdot) - \omega_{N_k}(f, \cdot)\|_{L^p(a, b)} \rightarrow 0 \quad \text{as } k \rightarrow \infty$$

for all $p \in [1, \infty)$. If f has further a continuous modulus of continuity, then there especially holds

$$\|\omega(f, \cdot) - \omega_{N_k}(f, \cdot)\|_{L^\infty(a, b)} \rightarrow 0 \quad \text{as } k \rightarrow \infty.$$

Proof. The case $p = \infty$ is Corollary 3.5. For $p \in [1, \infty)$, we distinguish two cases. For $a > 0$ we infer from Theorem 3.9 that

$$\|\omega(f, \cdot) - \omega_{N_k}(f, \cdot)\|_{L^p(a, b)} \leq 2^{(p-1)/p} \|\omega(f, \cdot) - \omega(f, \cdot - r_k)\|_{L^p(a, b)} + 2(b - a)^{1/p} \omega(f, r_k).$$

Continuity of the shift operator in L^p implies that the first term tends to zero as $k \rightarrow \infty$, whereas the second term tends to zero due to Lemma 2.4.

For $a = 0$, we set $\alpha_k = \max\{r_k, b/k\} > 0$. Then $\alpha_k \rightarrow 0$ as $k \rightarrow \infty$ and $\{X_{N_k}\}_{k \in \mathbb{N}}$ is especially a sequence of $\alpha_k/2$ -nets. Employing Corollary 3.10, this implies

$$\begin{aligned} & \|\omega(f, \cdot) - \omega_{N_k}(f, \cdot)\|_{L^p(0, b)} \\ & \leq \alpha_k^{1/p} \omega(f, \alpha_k) + 2^{(p-1)/p} \|\omega(f, \cdot) - \omega(f, \cdot - \alpha_k)\|_{L^p(\alpha_k, b)} + 2(b - \alpha_k)^{1/p} \omega(f, \alpha_k). \end{aligned}$$

Therefore, a minor modification of the argument for $a > 0$ yields the assertion. \square

This consistency result is in line with what is to be expected. The discrete modulus of continuity is a piecewise constant function and piecewise constant functions are good approximants for discontinuous functions in $L^p(a, b)$, $p \in [1, \infty)$. This is not necessarily the case for $L^\infty(a, b)$, where we require the limit function to be continuous.

3.4 Consistency of the $|\cdot|_{\rho, N}$ -seminorm

Observing that the $|\cdot|_{\rho, N}$ -seminorm of f can be considered as a weighted version of the $\|\cdot\|_{L^\infty(0, T_{\mathcal{X}})}$ -norm of $\omega_N(f, \cdot)$, the following consistency result is an intuitive extension of Corollary 3.11. The only difficulty is a potential singularity of ρ^{-1} close to the origin.

Theorem 3.12 (Consistency of the $|\cdot|_{\rho, N}$ -seminorm). *Let $\omega(f, \cdot), \rho(\cdot)^{-1}\omega(f, \cdot): [0, \infty] \rightarrow [0, \infty)$ be continuous and $|f|_\rho < \infty$. Let $\{r_k\}_{k \in \mathbb{N}}$ be a non-increasing sequence with $\lim_{k \rightarrow \infty} r_k = 0$ and $X_{N_k} = \{\mathbf{x}_1, \dots, \mathbf{x}_{N_k}\} \subset \mathcal{X}$ be $r_k/2$ -nets of \mathcal{X} with $X_{N_k} \subset X_{N_{k+1}}$, $k \in \mathbb{N}$. Then, there holds*

$$\lim_{k \rightarrow \infty} |f|_{\rho, N_k} = \lim_{k \rightarrow \infty} |f|_{\rho, N_k} \rightarrow |f|_\rho, \quad \text{as } k \rightarrow \infty.$$

Proof. It follows from the definition that $|f|_{\rho, N_k}$ is non-decreasing in k and bounded from above by $|f|_\rho$. This yields $\lim_{k \rightarrow \infty} |f|_{\rho, N_k} \leq |f|_\rho$. We show by contradiction that the inequality is an equality. Assume that there exists $0 < M < |f|_\rho$ such that $|f|_{\rho, N_k} \leq M$ for all k . By the definition of the $|f|_\rho$ -seminorm, there is a sequence $\{t_j\}_{j \in \mathbb{N}} \subset \mathcal{Z} \setminus \{0\}$ with \mathcal{Z} as in Equation (14), such that

$$\lim_{j \rightarrow \infty} \rho(t_j)^{-1} \omega(f, t_j) = |f|_\rho.$$

Thus, there exists $J \in \mathbb{N}$ such that $\rho(t_J)^{-1} \omega(f, t_J) > M$.

Now, let $0 < \varepsilon < \rho(t_J)^{-1} \omega(f, t_J) - M$. Since $\rho(\cdot)^{-1}\omega(f, \cdot)$ is continuous, Lemma 3.4 implies that there is $k \in \mathbb{N}$ large enough such that $s \in Z_{N_k}$, with Z_{N_k} as in Equation (14), satisfies

$$|\rho(t_J)^{-1} \omega(f, t_J) - \rho(s)^{-1} \omega(f, s)| \leq \frac{\varepsilon}{2}.$$

Exploiting $Z_{N_k} \subset Z_{N_{k+\ell}}$ for $\ell \in \mathbb{N}$ and the continuity of $\omega(f, \cdot)$ as well as Lemma 2.4 and Theorem 3.6, we conclude that there further exists ℓ large enough such that

$$0 \leq \rho(s)^{-1} (\omega(f, s) - \omega_{N_{k+\ell}}(f, s)) \leq \rho(s)^{-1} (\omega(f, s) - \omega(f, s - r_{k+\ell}) + \omega(f, r_{k+\ell})) \leq \frac{\varepsilon}{2}.$$

The triangle inequality thus implies

$$|\rho(t_J)^{-1} \omega(f, t_J) - \rho(s)^{-1} \omega_{N_{k+\ell}}(f, s)| \leq \varepsilon.$$

Based on the previous bound together with the choice of $0 < \varepsilon < \rho(t_J)^{-1}\omega(f, t_J) - M$, we obtain

$$\begin{aligned}\rho(s)^{-1}\omega_{N_{k+\ell}}(f, s) &= \rho(s)^{-1}\omega_{N_{k+\ell}}(f, s) - \rho(t_J)^{-1}\omega(f, t_J) + \rho(t_J)^{-1}\omega(f, t_J) \\ &> -\varepsilon + \rho(t_J)^{-1}\omega(f, t_J) > M.\end{aligned}$$

This implies

$$|f|_{\rho, N_{k+\ell}} \geq \rho(s)^{-1}\omega_{N_{k+\ell}}(f, s) > M,$$

which is a contradiction to the assumption. \square

4 Consistency for empirical data sites

The following section is dedicated to consistency estimates for the discrete modulus of continuity for empirical data sites. Assuming that the data sites are drawn according to a probability distribution and that the site-to-value map $f_N: X_N \rightarrow Y_N$ is the restriction of a function $f: \mathcal{X} \rightarrow \mathcal{Y}$ we derive probabilistic estimates for the approximation of the modulus of continuity by the discrete one. Further, we discuss the consistency of the discrete modulus of continuity in the infinite sample limit, that is, $N \rightarrow \infty$. The additional requirement on \mathcal{X} compared to Section 3 is as follows.

Let $\mathcal{B} \subset 2^{\mathcal{X}}$ denote the Borel σ -field on \mathcal{X} . Throughout this section, we assume that the measurable space $(\mathcal{X}, \mathcal{B})$ is equipped with a probability measure $\mathbb{P}: \mathcal{B} \rightarrow [0, 1]$. Without loss of generality we assume that \mathbb{P} is nondegenerate, that is, all open neighborhoods of all elements in \mathcal{X} have positive measure. Throughout this section, we assume that the data sites in $X_N = \{\mathbf{x}_1, \dots, \mathbf{x}_N\}$ have been drawn independently according to \mathbb{P} .

4.1 Random coverings

The following two standard results are important ingredients to prove the consistency of the discrete modulus of continuity for empirical data sites. We state here for the reader's convenience.

Lemma 4.1 (Positive probability of balls). *There holds*

$$\inf_{\mathbf{x} \in \mathcal{X}} \mathbb{P}(B_r(\mathbf{x})) > 0$$

for all $r > 0$.

Proof. We prove the claim by contradiction. Assume that there exists an $r > 0$ such that $\inf_{\mathbf{x} \in \mathcal{X}} \mathbb{P}(B_r(\mathbf{x})) = 0$. Then, there exists a minimizing sequence $\{\mathbf{x}_n\}_{n \in \mathbb{N}} \subset \mathcal{X}$ such that

$$\lim_{n \rightarrow \infty} \mathbb{P}(B_r(\mathbf{x}_n)) = \inf_{\mathbf{x} \in \mathcal{X}} \mathbb{P}(B_r(\mathbf{x})) = 0.$$

Since \mathcal{X} is compact, the minimizing sequence $\{\mathbf{x}_n\}_{n \in \mathbb{N}}$ has a convergent subsequence $\{\mathbf{x}_{\varphi(n)}\}_{n \in \mathbb{N}}$ with limit $\mathbf{x}^* \in \mathcal{X}$. There holds

$$\lim_{n \rightarrow \infty} \mathbb{P}(B_r(\mathbf{x}_{\varphi(n)}) \cap B_r(\mathbf{x}^*)) \leq \lim_{n \rightarrow \infty} \mathbb{P}(B_r(\mathbf{x}_{\varphi(n)})) = 0. \quad (19)$$

Furthermore, we have for each $\mathbf{x} \in B_r(\mathbf{x}_{\varphi(n)})$ that

$$d_{\mathcal{X}}(\mathbf{x}, \mathbf{x}^*) \leq d_{\mathcal{X}}(\mathbf{x}, \mathbf{x}_{\varphi(n)}) + d_{\mathcal{X}}(\mathbf{x}_{\varphi(n)}, \mathbf{x}^*) \leq r + \varepsilon(n),$$

where we set $\varepsilon(n) := d_{\mathcal{X}}(\mathbf{x}_{\varphi(n)}, \mathbf{x}^*)$. This implies the inclusion $B_r(\mathbf{x}_{\varphi(n)}) \subset B_{r+\varepsilon(n)}(\mathbf{x}^*)$ and, therefore, $B_r(\mathbf{x}_{\varphi(n)}) \cap B_r(\mathbf{x}^*) \rightarrow B_r(\mathbf{x}^*)$ for $n \rightarrow \infty$, since $\varepsilon(n) \rightarrow 0$. By the continuity of \mathbb{P} from below and its nondegeneracy on \mathcal{X} , we conclude

$$\lim_{n \rightarrow \infty} \mathbb{P}(B_r(\mathbf{x}_{\varphi(n)}) \cap B_r(\mathbf{x}^*)) = \mathbb{P}(B_r(\mathbf{x}^*)) > 0.$$

This is a contradiction to Equation (19). \square

Lemma 4.2 (Covering probability). *For any $r \geq 0$, there holds*

$$\mathbb{P}\left(\bigcup_{n=1}^N B_r(\mathbf{x}_n) = \mathcal{X}\right) \geq P(r, N)$$

with

$$P(r, N) := 1 - \mathcal{N}(\mathcal{X}, r/2)\eta(r/2)^N, \quad \eta(r) := \sup_{\mathbf{x} \in \mathcal{X}} (1 - \mathbb{P}(B_r(\mathbf{x}))) < 1. \quad (20)$$

Proof. From Lemma 4.1, we directly infer that $\eta(r) < 1$. Further, by definition of the covering number, we know that there exist $\mathcal{N}(\mathcal{X}, r/2)$ balls $B_{r/2}(\mathbf{x}'_n)$, $n = 1, \dots, \mathcal{N}(\mathcal{X}, r/2)$, covering \mathcal{X} . This implies by the Bonferroni inequality that

$$\begin{aligned} \mathbb{P}\left(\bigcup_{n=1}^N B_r(\mathbf{x}_n) = \mathcal{X}\right) &\geq \mathbb{P}(X_N \cap B_{r/2}(\mathbf{x}'_n) \neq \emptyset \text{ for } n = 1, \dots, \mathcal{N}(\mathcal{X}, r/2)) \\ &\geq 1 - \sum_{n=1}^{\mathcal{N}(\mathcal{X}, r/2)} \mathbb{P}(X_N \cap B_{r/2}(\mathbf{x}'_n) = \emptyset). \end{aligned}$$

Now, since the points $\mathbf{x}_1, \dots, \mathbf{x}_N$ are independent realizations we obtain

$$\mathbb{P}(X_N \cap B_{r/2}(\mathbf{x}'_n) = \emptyset) = \left(1 - \mathbb{P}(B_{r/2}(\mathbf{x}'_n))\right)^N \leq \eta(r/2)^N$$

for any $n = 1, \dots, \mathcal{N}(\mathcal{X}, r)$. Inserting this bound into the previous estimate yields the assertion. \square

The following straightforward monotonicity result will be helpful later on.

Lemma 4.3 (Covering probabilities are monotonically increasing). *Let $N \in \mathbb{N}$. Then there holds*

$$P(r, N) \leq P(r', N) \leq 1$$

for all $0 \leq r \leq r'$.

Remark 4.4. *Lemmas 4.2 and 4.3 formalize what is intuitively clear: For fixed N , the probability of covering \mathcal{X} with N balls of radius r decreases when r decreases. Vice versa, for fixed r , the probability of covering \mathcal{X} with N balls with radius r increases for increasing N .*

4.2 Pointwise consistency

The following theorem connects the deterministic pointwise approximation result from Theorem 3.6 with the probability that the empirical data sites satisfy the required $r/2$ -net property.

Theorem 4.5 (Consistency in probability for fixed t). *Let $f: \mathcal{X} \rightarrow \mathcal{Y}$ have continuous modulus of continuity. Then, $\omega_N(f, t)$ converges to $\omega(f, t)$ in probability for all $t \geq 0$, that is, for all $\varepsilon > 0$, there holds*

$$\lim_{N \rightarrow \infty} \mathbb{P}(\omega(f, t) - \omega_N(f, t) \leq \varepsilon) = 1 \quad \text{for all } t \geq 0.$$

More precisely, for all $t \geq 0$ there exists $r \in (0, t]$, which only depends on $\omega(f, \cdot)$ and t , such that

$$\mathbb{P}(\omega(f, t) - \omega_N(f, t) \leq \varepsilon) \geq \mathbb{P}\left(\bigcup_{n=1}^N B_{r/2}(\mathbf{x}_n) = \mathcal{X}\right) \geq P(r/2, N). \quad (21)$$

Proof. The result for $t = 0$ follows trivially. Hence, let $t > 0$. Since $\omega(f, \cdot)$ is continuous there exists for every $\varepsilon > 0$ an $r \in (0, t]$ such that

$$\omega(f, t) - \omega(f, t - r) \leq \frac{\varepsilon}{3}, \quad \omega(f, r) \leq \frac{\varepsilon}{3}.$$

Theorem 3.6 thus implies

$$0 \leq \omega(f, t) - \omega_N(f, t) \leq \omega(f, t) - \omega(f, t - r) + 2\omega(f, r) \leq \varepsilon$$

for all sets of data sites X_N which form an $r/2$ -net. Estimate (21) follows now with Lemma 4.2 and implies in view of in Equation (20) convergence in probability. \square

Based on the pointwise consistency result in probability, consistency results in $L_{\mathbb{P}}^s(\mathcal{X})$ and \mathbb{P} -almost sure consistency for fixed t can be readily deduced as follows.

Corollary 4.6 (Consistency of moments for fixed t). *Under the assumptions of Theorem 4.5, there holds for all $t \geq 0$, $s \in [1, \infty)$ that*

$$\lim_{N \rightarrow \infty} \mathbb{E}[|\omega(f, t) - \omega_N(f, t)|^s] = 0.$$

Proof. It is sufficient to show that $\omega_N(f, t)$ is uniformly integrable over \mathcal{X} , see, for example, [23, Exercise 6.15]. This is trivially fulfilled, since Lemma 2.7 implies that

$$\mathbb{E}[|\omega_N(f, t)|^s] \leq \mathbb{E}[|\omega(f, t)|^s] = |\omega(f, t)|^s$$

for all $s \in [1, \infty)$. \square

Corollary 4.7 (\mathbb{P} -almost sure consistency for fixed t). *Under the assumptions of Theorem 4.5, and for all $t \geq 0$, $\omega_N(f, t)$ converges to $\omega(f, t)$ \mathbb{P} -almost surely, that is,*

$$\mathbb{P}\left(\lim_{N \rightarrow \infty} \omega_N(f, t) = \omega(f, t)\right) = 1.$$

Proof. The consistency in probability, as shown in Theorem 4.5, implies that there exists a subsequence $\omega_{N_k}(f, t)$ which converges almost surely to $\omega(f, t)$, that is,

$$\mathbb{P}\left(\lim_{k \rightarrow \infty} \omega_{N_k}(f, t) = \omega(f, t)\right) = 1,$$

see, for example, [23, Theorem 2.30]. The monotonicity of $\omega_N(f, t)$ in N , see Lemma 2.7, now implies the assertion. \square

4.3 Consistency on intervals

In analogy to the deterministic case, the following results inspect the consistency in $L^p(a, b)$.

Theorem 4.8 (Consistency in probability in $L^p(a, b)$). *Let $[a, b] \subset [0, T_{\mathcal{X}}]$. Let $f: \mathcal{X} \rightarrow \mathcal{Y}$ be continuous for $p \in [1, \infty)$ and let f have continuous modulus of continuity for $p = \infty$. Then, for all $p \in [1, \infty]$, we have $\|\omega_N(f, \cdot) - \omega(f, \cdot)\|_{L^p(a, b)} \rightarrow 0$ in probability, that is, for all $\varepsilon > 0$, there holds*

$$\lim_{N \rightarrow \infty} \mathbb{P}(\|\omega(f, \cdot) - \omega_N(f, \cdot)\|_{L^p(a, b)} \leq \varepsilon) = 1.$$

More precisely, for each interval $[a, b]$, there exists $r \in (0, b]$, which only depends on $\omega(f, \cdot)$ and $[a, b]$, such that

$$\mathbb{P}(\|\omega(f, \cdot) - \omega_N(f, \cdot)\|_{L^p(a, b)} \leq \varepsilon) = \mathbb{P}\left(\bigcup_{n=1}^N B_{r/2}(\mathbf{x}_n) = \mathcal{X}\right) \geq P(r/2, N).$$

Proof. Without loss of generality we can assume that $a = 0$. In this case, we have for all $\alpha \in [0, b]$ that

$$\|\omega(f, \cdot) - \omega_N(f, \cdot)\|_{L^p(0, b)} \leq \|\omega(f, \cdot) - \omega_N(f, \cdot)\|_{L^p(0, \alpha)} + \|\omega(f, \cdot) - \omega_N(f, \cdot)\|_{L^p(\alpha, b)}.$$

In analogy to the proof of Corollary 3.10 the first term on the right-hand side can be estimated by

$$\|\omega(f, \cdot) - \omega_N(f, \cdot)\|_{L^p(0, \alpha)} \leq \|\omega(f, \cdot)\|_{L^p(0, \alpha)} \leq \begin{cases} \alpha^{1/p} \omega(f, \alpha), & p \in [1, \infty), \\ \omega(f, \alpha), & p = \infty. \end{cases}$$

Now, for fixed $\varepsilon > 0$, we choose $0 < \alpha \leq b$ such that $\alpha^{1/p} \omega(f, \alpha) < \varepsilon/2$ for $p \in [1, \infty)$ or $\omega(f, \alpha) < \varepsilon/2$ for $p = \infty$. Then, we obtain the bound

$$\|\omega(f, \cdot) - \omega_N(f, \cdot)\|_{L^p(0, b)} \leq \frac{\varepsilon}{2} + \|\omega(f, \cdot) - \omega_N(f, \cdot)\|_{L^p(\alpha, b)},$$

which holds \mathbb{P} -almost surely. It remains to show that

$$\mathbb{P}\left(\|\omega(f, \cdot) - \omega_N(f, \cdot)\|_{L^p(\alpha, b)} \leq \frac{\varepsilon}{2}\right) \rightarrow 1, \quad N \rightarrow \infty.$$

For $p \in [1, \infty)$ continuity of the shift operator and Lemma 2.4 imply that there exists $r \in (0, \alpha]$ such that

$$2^{(p-1)/p} \|\omega(f, \cdot) - \omega(f, \cdot - r)\|_{L^p(\alpha, b)} + 2(b - \alpha)^{1/p} \omega(f, r) \leq \frac{\varepsilon}{2}.$$

Further, since we consider the limit $N \rightarrow \infty$ and since \mathcal{X} is compact, we can assume that $N \geq \mathcal{N}(\mathcal{X}, r/2)$. Then, Theorem 3.9 implies that

$$\begin{aligned}
& \mathbb{P}\left(\|\omega(f, \cdot) - \omega_N(f, \cdot)\|_{L^p(\alpha, b)} \leq \frac{\varepsilon}{2}\right) \\
& \geq \mathbb{P}\left(2^{(p-1)/p} \|\omega(f, \cdot) - \omega(f, \cdot - r)\|_{L^p(\alpha, b)} + 2(b - \alpha)^{1/p} \omega(f, r) \leq \frac{\varepsilon}{2}\right) \\
& \geq \mathbb{P}\left(\bigcup_{n=1}^N B_{r/2}(\mathbf{x}_n) = \mathcal{X}\right) \\
& \geq P(r/2, N) \\
& \rightarrow 1
\end{aligned}$$

as $N \rightarrow \infty$. The assertion for $p = \infty$ follows in complete analogy, using the corresponding bound from Theorem 3.9 for this case. \square

Consistency results in $L_{\mathbb{P}}^s(\mathcal{X})$ and \mathbb{P} -almost sure consistency on intervals are an immediate consequence of the previous theorem.

Corollary 4.9 (Consistency of moments in $L^p(a, b)$). *Under the assumptions of Theorem 4.8, there holds $\|\omega(f, \cdot) - \omega_N(f, \cdot)\|_{L^p(a, b)} \rightarrow 0$ in $L_{\mathbb{P}}^s(\mathcal{X})$ for any $p \in [1, \infty]$ and any $s \in [1, \infty)$, that is,*

$$\lim_{N \rightarrow \infty} \left(\mathbb{E}[\|\omega(f, \cdot) - \omega_N(f, \cdot)\|_{L^p(a, b)}^s] \right)^{1/s} = 0.$$

Proof. The proof is in analogy to Corollary 4.6. \square

Corollary 4.10 (\mathbb{P} -almost sure consistency in $L^p(a, b)$). *Under the assumptions of Theorem 4.8, and with $p \in [1, \infty]$, the sequence $\|\omega(f, \cdot) - \omega_N(f, \cdot)\|_{L^p(a, b)} \rightarrow 0$ converges almost surely, that is,*

$$\mathbb{P}\left(\lim_{N \rightarrow \infty} \|\omega(f, \cdot) - \omega_N(f, \cdot)\|_{L^p(a, b)} = 0\right) = 1.$$

Proof. The assertion follows similarly to the proof of Corollary 4.7. \square

4.4 Consistency of the empirical $|\cdot|_{\rho, N}$ -seminorm

The consistency of the $|\cdot|_{\rho, N}$ -seminorm for empirical data sites follows directly from the deterministic case.

Theorem 4.11 (Consistency of the empirical $|\cdot|_{\rho, N}$ -seminorm). *Let $\rho(\cdot)^{-1}\omega(f, \cdot) : [0, \infty] \rightarrow [0, \infty)$ be continuous and $|f|_{\rho} < \infty$. Then, there holds*

$$\lim_{N \rightarrow \infty} |f_N|_{\rho, N} = \lim_{N \rightarrow \infty} |f|_{\rho, N} = |f|_{\rho}$$

\mathbb{P} -almost surely.

Proof. We first show by contradiction that the fill distance h_{X_N} , see Equation (3), of N random, independently drawn points on \mathcal{X} converges to zero \mathbb{P} -almost surely for $N \rightarrow \infty$. Assume that $h_{X_N} \geq h_0 > 0$ for all $N \in \mathbb{N}$. Then, there exists $\mathbf{x} \in \mathcal{X}$ such that $\emptyset = B_{h_0}(\mathbf{x}) \cap \{\mathbf{x}_i\}_{i=1}^N$ for all $N \in \mathbb{N}$. By the same argumentation as in the proof of Lemma 4.2, the probability of this being the case is bounded by

$$\mathbb{P}\left(\{\mathbf{x}_i\}_{i=1}^N \cap B_{h_0}(\mathbf{x}) = \emptyset\right) \leq \eta(h_0)^N$$

with $\eta(h_0) < 1$ defined as in Equation (20). For $N \rightarrow \infty$, this probability goes to zero, meaning that with probability 1 there exists $i \in \mathbb{N}$ such that $\mathbf{x}_i \in B_{h_0}(\mathbf{x})$. This is a contradiction to h_0 being a lower bound to the fill distance for all $N \in \mathbb{N}$.

Hence, we infer that the family of balls $\{B_{h_{X_N}}(\mathbf{x}_i)\}_{i=1}^N$ generates a sequence of h_{X_N} -nets on \mathcal{X} and the assumptions of Theorem 3.12 are satisfied \mathbb{P} -almost surely with $r_k/2 = h_{X_N}$. This implies the assertion. \square

5 Computation of the discrete modulus of continuity

The computation of the discrete modulus of continuity from Equation (6), that is,

$$\omega_N(f, t) = \max_{\substack{\mathbf{x}_i, \mathbf{x}_j \in X_N: \\ d_{i,j} \leq t}} d_{\mathcal{Y}}(f(\mathbf{x}_i), f(\mathbf{x}_j)),$$

requires the evaluation of the distances $d_{\mathcal{Y}}(f(\mathbf{x}_i), f(\mathbf{x}_j))$ for all $i, j = 1, \dots, N$. Therefore, the computational cost is $\mathcal{O}(N^2)$. The same is true if we aim at computing the discrete seminorm $|f|_{\rho, N}$, see Equations (9) and (10), from data. Fortunately, for sufficiently small values of t , the computational cost can be reduced if the metric space \mathcal{X} exhibits sufficient structure and if we restrict the evaluation of $d_{\mathcal{Y}}(f(\mathbf{x}_i), f(\mathbf{x}_j))$ to pairs of data sites $(\mathbf{x}_i, \mathbf{x}_j)$ with distance smaller than a fixed t . If such structure is present, the latter can efficiently be realized using an ε -nearest neighbor search.

Based on this consideration, we provide a heuristic algorithm for the efficient evaluation of the modulus of continuity. This heuristic is based on two further observations. The first observation is that the modulus of continuity is monotonically increasing, see Lemma 2.4. The second observation is that, for our applications, we require an accurate approximation of the modulus of continuity only close to the zero, where its magnitude is typically small. Less precise approximations are acceptable for increasing distance from zero. In the following, we first recall the efficient implementation of the ε -nearest neighbor search as well as a coarsening strategy for set covers. Afterwards, we discuss the details of our algorithm for the efficient evaluation of the modulus of continuity.

5.1 ε -nearest neighbor search

For an efficient implementation of the search for nearest neighbors, further assumptions on the structure of the metric space $(\mathcal{X}, d_{\mathcal{X}})$ are required, compare Example 3.3.

Definition 5.1. Let $(\mathcal{X}, d_{\mathcal{X}})$ be a metric space.

1. The space $(\mathcal{X}, d_{\mathcal{X}})$ is Ahlfors n -regular, if there exists a Borel regular measure μ and constants $C \geq 1$, $n > 0$ such that

$$C^{-1}R^n \leq \mu(B_R(\mathbf{x})) \leq CR^n$$

for all $\mathbf{x} \in \mathcal{X}$, $R > 0$.

2. The space $(\mathcal{X}, d_{\mathcal{X}})$ is (C, s) -homogeneous, if

$$\mathcal{N}(B_R(\mathbf{x}), r) \leq C \left(\frac{R}{r} \right)^s$$

for all $\mathbf{x} \in \mathcal{X}$ and all $0 < r < R < \infty$. The infimum of the set of all s such that $(\mathcal{X}, d_{\mathcal{X}})$ is (C, s) -homogeneous is the Assouad dimension of $(\mathcal{X}, d_{\mathcal{X}})$.

3. The space $(\mathcal{X}, d_{\mathcal{X}})$ has bounded doubling dimension if there exists $0 \leq s < \infty$ such that

$$\mathcal{N}(B_r(\mathbf{x}), r/2) \leq 2^s$$

for all $\mathbf{x} \in \mathcal{X}$ and any $r > 0$. We refer to the infimum over all s such that the bound holds as the doubling dimension of $(\mathcal{X}, d_{\mathcal{X}})$.

A bounded Assouad dimension is equivalent to a bounded doubling dimension, see, for example, [31]. For the particular case of an Ahlfors n -regular space, however, the Assouad dimension and the doubling dimension are both equal to n .

For the purpose of deriving cost bounds of the ε -nearest neighbor search, it is assumed in literature that $(\mathcal{X}, d_{\mathcal{X}})$ has bounded doubling dimension s . The cost for the ε -nearest neighbor search of a given point $\mathbf{x} \in X_N$ is then bounded by $2^{cs}(\log \Delta + |B_{C\varepsilon}(\mathbf{x}) \cap X_N|)$ for two constants $c, C > 0$, where $\Delta := \text{diam}(X_N)/q_{X_N}$ is the aspect ratio of X_N , see [6, 38], and q_{X_N} is the separation distance, see Equation (4).

Remark 5.2. Let $X_N \subset \mathcal{X}$ a quasi-uniform set of data sites, see Equation (5), in an Ahlfors n -regular metric space \mathcal{X} . Especially, the doubling dimension equals n in this case. Using a volume argument it is easy to show that $c^{-1}N^{-1/n} \leq q_{X_N} \leq cN^{-1/n}$ for some $c > 0$. This implies

$$\Delta = \mathcal{O}(N^{1/n}), \quad |B_\varepsilon(\mathbf{x}) \cap X_N| = \mathcal{O}((\varepsilon/q_{X_N})^n) = \mathcal{O}(\varepsilon^n N).$$

Therefore, the cost of finding the ε -nearest neighbors for each $\mathbf{x} \in X_N$ is $\mathcal{O}(N(\log N + \varepsilon^n N))$ with the constant depending on the quasi-uniformity constant and the Ahlfors regularity, measure, and constant. For the choice $\varepsilon = \mathcal{O}(N^{-1/n} \log^{1/n}(N))$ the cost becomes $\mathcal{O}(N \log N)$.

The data structure for the efficient ε -nearest neighbor search can be organized as a *cluster tree*, see, for example, [27].

Definition 5.3. A cluster tree \mathcal{T} for X_N is a tree whose vertices correspond to non-empty subsets of X_N and are referred to as clusters. We require that the root of \mathcal{T} corresponds to X_N and that it holds $\dot{\cup}_{\tau' \in \text{children}(\tau)} \tau' = \tau$ for all non-leaf clusters, that is, $\text{children}(\tau) \neq \emptyset$. Furthermore, we introduce the set of leaf clusters $\mathcal{L} := \{\tau \in \mathcal{T} : \text{children}(\tau) = \emptyset\}$. The level $\ell(\tau)$ of $\tau \in \mathcal{T}$ is its distance from the root.

While cluster trees can be constructed on any metric space with finite doubling dimension, algorithms and complexity estimates can become quite technical. For simplicity we restrict ourselves in the following to quasi-uniform data sets in Ahlfors n -regular spaces. In this setting, we can simply consider *uniform n -d-trees*.

Definition 5.4. Let \mathcal{T} be a cluster tree for $X_N \subset \mathcal{X}$. We call \mathcal{T} an n -d-tree, if each non-leaf cluster has exactly $2^{\lceil n \rceil}$ children, that is, $|\text{children}(\tau)| = 2^{\lceil n \rceil}$ for all $\tau \in \mathcal{T} \setminus \mathcal{L}$. It is a balanced n -d-tree, if it is an n -d-tree and there is some $c_b > 0$ such that it holds

$$c_b^{-1} 2^{J - \lceil n \rceil \ell(\tau)} \leq |\tau| \leq c_b 2^{J - \lceil n \rceil \ell(\tau)}$$

for all $\tau \in \mathcal{T}$. Finally, \mathcal{T} is a uniform n -d-tree if it is a balanced n -d-tree and

$$c_{\text{diam}}^{-1} 2^{-c_{\text{uni}} \ell(\tau)} \leq \text{diam}(\tau) \leq c_{\text{diam}} 2^{-c_{\text{uni}} \ell(\tau)}$$

for all clusters $\tau \in \mathcal{T}$ and some constants $c_{\text{diam}}, c_{\text{uni}} > 0$.

Remark 5.5. If $X_N \subset \Omega$ for some region $\Omega \subset \mathbb{R}^k$ endowed with a norm, then a balanced k -d-tree can be obtained by successively subdividing the bounding box B_τ , that is, the smallest axis-parallel cuboid that contains all points, of a given cluster τ into 2^k congruent cuboids. If X_N is quasi-uniform, this even yields a uniform k -d-tree, see, for example, [30]. The cost for this algorithm is then $\mathcal{O}(N \log N)$. For general metric spaces, graph-based clustering approaches may be employed to construct a cluster tree based on nested $2^{-\ell}$ -nets leading to navigating nets as in [38].

For illustrative purposes we recall the ε -nearest neighbor algorithm for the case when a cluster tree on X_N is available in Algorithm 1. For practical applications we may replace the criterion $\text{dist}_\mathcal{X}(\tau', \mathbf{x}) - \text{diam}_\mathcal{X}(\tau') < \varepsilon$ by an upper estimate using bounding boxes or spheres if applicable, see, for example, [27]. For the more general case we refer to [38].

5.2 Algorithms for the set cover problem

Given the sets of data sites X_N and the set of data values Y_N , the ε -nearest neighbor search from the previous paragraph allows for the computation of the discrete modulus of continuity with cost $\mathcal{O}(N(\log N + t^n N))$ within the setting of Remark 5.2. This allows for the efficient computation of the modulus of continuity for small values of t . For larger values, the cost of evaluating the modulus of continuity easily becomes $\mathcal{O}(N^2)$ and, thus, computationally prohibitive for large values of N . Within this section, we shall devise a coarsening strategy to mitigate this computational burden.

The key observation is that an $r/2$ -covering of X_N is sufficient to approximate $\omega_N(f_N, t)$ up to an accuracy of $\omega_N(f_N, t) - \omega_N(f_N, t-r) + 2\omega_N(f_N, r)$ for all $t \geq r$, see Theorem 3.6. Therefore, if we can coarsen the set X_N to a subset $X_{N'} \subset X_N$, $|X_{N'}| = N'$, whose elements are the centers of an $r/2$ -covering of X_N , we can evaluate $\omega_{N'}(f(f_{N'}, t) \approx \omega_N(f_N, t)$ up to an accuracy of $\omega_N(f_N, t) - \omega_N(f_N, t-r) + 2\omega_N(f_N, r)$ with computational cost $\mathcal{O}((N')^2)$. This approach yields a

Algorithm 1 ε -nearest neighbor algorithm based on cluster trees

Input: cluster tree \mathcal{T} on X_N , $\mathbf{x} \in X_N$, $\varepsilon > 0$
Output: $\mathcal{R} = B_\varepsilon(\mathbf{x}) \cap X_N$
Set $\mathcal{Q} = \{\text{root}(\mathcal{T})\}$, $\mathcal{R} = \emptyset$
while $\mathcal{Q} \neq \emptyset$ **do**
 Select the last element τ that has been added to \mathcal{Q} and set $\mathcal{Q} = \mathcal{Q} \setminus \{\tau\}$
 if $\text{children}(\tau) = \emptyset$ **then**
 Set $\mathcal{R} = \mathcal{R} \cup (\{\tau\} \cap B_\varepsilon(\mathbf{x}))$
 else
 for $\tau' \in \text{children}(\tau)$ **do**
 if $\text{dist}_{\mathcal{X}}(\tau', \mathbf{x}) - \text{diam}_{\mathcal{X}}(\tau') < \varepsilon$ **then**
 Set $\mathcal{Q} = \mathcal{Q} \cup \{\tau'\}$
 end if
 end for
 end if
end while
return \mathcal{R}

reasonable approximation as long as $\omega_N(f_N, t) - \omega_N(f_N, t-r)$ is small. This is the case if $\omega_N(f_N, t)$ behaves reasonably in a vicinity of t .

We note that finding an optimal coarsening corresponds to the *set cover problem*, which is well known to be NP-hard. It has been subject to intense research efforts for polynomial approximation algorithms and we refer to [37, 49] for reviews. A particular greedy strategy from [10] for its approximate solution is given in Algorithm 2. An efficient implementation of Algorithm 2 based

Algorithm 2 Greedy algorithm for set cover problem, see [10].

Input: Set of data sites X_N , radius $r/2 > 0$
Output: $X_{N'} \subset X_N$, $|X_{N'}| = N'$, such that $X_N \subset \bigcup_{\mathbf{x} \in X_{N'}} B_{r/2}(\mathbf{x})$
Set $X_{N'} = \emptyset$, $Z = X_N$
while $Z \neq \emptyset$ **do**
 Compute $S_j = B_{r/2}(\mathbf{x}_j) \cap Z$, $j = 1, \dots, N$
 Set $j = \text{argmax}\{j = 1, \dots, N : |S_j|\}$
 Set $X_{N'} = X_{N'} \cup \mathbf{x}_j$
 Set $Z = Z \setminus S_j$
end while
return $X_{N'}$

on boolean lists requires only a single precomputation of the sets S_j , see, for example, [4]. The number of steps performed by the greedy strategy is N' . Moreover, it returns an

$$H(N) = \sum_{k=1}^N \frac{1}{k} \leq \log(N) + 1$$

optimal covering, in the sense that $N' \leq H(N) \cdot \mathcal{N}(X_N, r/2)$. Up to lower order terms this bound is optimal, see [46].

If a binary max-heap is used for the organization of the sets S_j , where the keys are the current cardinalities $|S_j|$, the maximum can be retrieved with cost $\mathcal{O}(1)$. For constructing such a heap the cost is $\mathcal{O}(N)$ when using the **heapify** operation, see, e.g., [13], which has to be done before the while loop. Each iteration of the while loop further entails one **pop** operation with cost at most $\log N$ and, assuming that $r = \mathcal{O}(q_{X_N})$ and X_N is quasi-uniform, $\mathcal{O}((r/2)^n)$ **decreaseKey** operations also of cost at most $\log N$. In view of $N' \leq H(N) \cdot \mathcal{N}(X_N, r/2)$ and $\mathcal{N}(X_N, r/2) = \mathcal{O}((r/2)^{-n})$, see Example 3.3.2, this leads to an overall cost of

$$\mathcal{O}(\mathcal{N}(X_N, r/2)(r/2)^n N \log^2 N) = \mathcal{O}(N \log^2 N) + \text{precomputation of } S_j \quad (22)$$

for Algorithm 2. For the precise cost for the precomputation of the S_j using the ε -nearest neighbor search, we refer to Section 5.1.

Depending on the size of the covering number, the coarsening step may result in a significant reduction of the computational cost for the evaluation of the discrete modulus of continuity, if we are willing to invest a certain margin of error. We recall that the value of the covering number depends on the geometry of $(\mathcal{X}, d_{\mathcal{X}})$, see Section 3.1. In the following, we further decrease the computational cost by employing an iterative coarsening procedure.

5.3 Efficient approximation of the discrete modulus of continuity

The algorithm we are going to introduce in a moment is based on the idea that the (discrete) modulus of continuity is a monotonically increasing function with $\omega(f, 0) = 0$. Since every modulus of continuity has a concave majorant, the values of the modulus of continuity close to $t = 0$ are of particular importance for a good approximation. This is exactly the regime where the ε -nearest neighbor search allows us to efficiently evaluate the discrete modulus of continuity exactly. In contrast, with increasing distance from $t = 0$, the modulus of continuity remains either constant or is increasing. If the modulus of continuity is constant, then its value has already been captured for a smaller value of t and a lower computational cost. If it is increasing, then we transition to a coarser covering, resulting in less data points to consider and thus lower computational cost with an approximation error that is dependent on the behavior of the modulus of continuity.

In the following, in Algorithms 3 and 4, we provide an approach, which takes the preceding considerations into account. We have divided it into an offline-online approach to allow for the

Algorithm 3 Offline phase for the efficient evaluation of the modulus of continuity.

Input: Set of data sites X_N , initial radius $r > 0$, growth factor $R > 1$, upper bound $T \leq T_{\mathcal{X}}$
Output: $\omega_{N_k}(Y_N, R^k r)$, $k = 0, \dots, K - 1$,
 sets $X_{N_0} \supseteq X_{N_1} \supseteq \dots \supseteq X_{N_{K-1}}$ with $|X_{N_k}| = N_k$, $k = 0, \dots, K - 1$
 Set $X_{N_0} = X_N$, $K = \lceil \log_R(T/r) \rceil$
 Optional: Set $X_{\min, \max} = \{\mathbf{x}_i, \mathbf{x}_j\}$ with $(i, j) \in \operatorname{argmax} \{(i, j) \in \{1, \dots, N\}^2 : d_{\mathcal{Y}}(\mathbf{y}_i, \mathbf{y}_j)\}$
for $k = 0, \dots, K - 1$ **do**
 Optional: Set $X_{N_k} = X_{N_k} \cup X_{\min, \max}$
 Compute $\omega_{N_k}(Y_{N_k}, R^k r)$ using an ε -nearest neighbor search with $\varepsilon = R^k r$
 Find an $R^k r$ -cover $X_{N_{k+1}}$ of X_{N_k} using Algorithm 2
end for
return $X_{N_k}, \omega_{N_k}(Y_{N_k}, R^k r)$, $k = 0, \dots, K - 1$

Algorithm 4 Online phase for the efficient evaluation of the modulus of continuity.

Input: Evaluation point $t \in [0, T]$, inputs and outputs from Algorithm 3
Output: Approximate value of $\omega_N(Y_N, t)$
if $t \in [0, r]$ **then**
 Compute $\omega_{N_0}(Y_N, t)$ on X_{N_0} using an ε -nearest neighbor search with $\varepsilon = t$
 return $\omega_{N_0}(Y_{N_0}, t) = \omega_N(Y_N, t)$
else
 Let $k \in \mathbb{N}$ such that $t \in (R^{k-1}r, R^k r]$
 Compute $\omega_{N_k}(Y_{N_k}, t)$ on X_{N_k} using an ε -nearest neighbor search with $\varepsilon = t$
 return $\max \{\omega_{N_k}(Y_{N_k}, t), \max_{\ell=0, \dots, k-1} \{\omega_{N_{\ell}}(Y_{N_{\ell}}, R^{\ell} r)\}\} \approx \omega_N(Y_N, t)$
end if

repeated evaluation for various values of t with minimal computational overhead. It is clear that the two algorithms can be merged if only a single approximate evaluation of the discrete modulus of continuity is required. The optional step of computing and including $X_{\min, \max}$ can be expensive, depending on the structure of Y_N , and is not strictly necessary. However, if it is efficiently computable, for example, if $Y_N \subset \mathbb{R}$, then it can have a large positive effect on the approximation quality. The reason for this is that Algorithm 4 only relies on coarsened sets for evaluating $\omega(Y_N, t)$ for larger values of t , where only larger values of $d_{\mathcal{Y}}(\mathbf{y}_i, \mathbf{y}_j)$ are relevant. By incorporating the data sites $X_{\min, \max}$ causing extremal function values, we more accurately capture the values of $d_{\mathcal{Y}}(\mathbf{y}_i, \mathbf{y}_j)$ on the coarsened grids, thus improving the approximation.

To avoid technicalities in the following result on the cost, we assume without loss of generality that $T_{\mathcal{X}} \leq 1$, that is, the aspect ratio satisfies $\Delta = T_{\mathcal{X}}/q_{X_N} \leq q_{X_N}^{-1}$. Otherwise, the result holds

by a suitable rescaling of the involved quantities.

Theorem 5.6 (Computational cost of Algorithm 3). *Assume that $(\mathcal{X}, d_{\mathcal{X}})$ is an Ahlfors n -regular metric space and let the set of data sites X_N be quasi-uniform. Then, for $R \geq 1$ and $r \approx q_{X_N} \approx N^{-1/n}$, the cost of Algorithm 3 is*

$$\mathcal{O}(R^{n(4-\lceil \log_R(T_{\mathcal{X}} \cdot N^{1/n}) \rceil)} N \log^3 N).$$

with a constant independent of r, R , and N .

Proof. We first recall that, in an Ahlfors n -regular metric space, the ε -nearest neighbor search for all points can be performed with cost $\mathcal{O}(N(\log N + \varepsilon^n N))$, see Remark 5.2. For each fixed point, the cost for computing the modulus of continuity is $\mathcal{O}(\varepsilon^n N)$. Therefore, the cost of computing $\omega_N(Y_N, \varepsilon)$ based on the ε -nearest neighbor search is of order

$$\mathcal{O}(N(\log N + \varepsilon^n N)).$$

Furthermore, Ahlfors n -regularity implies Assouad dimension n . Thus, the $\log(N)$ -optimality of Algorithm 2 and Equation (13) imply that finding an ε -covering entails a cost of order

$$\mathcal{O}(N \log^2 N + N(\log N + \varepsilon^n N)).$$

see Equation (22). Combining these two costs yields an overall cost of

$$\mathcal{O}(N(\log^2 N + \varepsilon^n N)). \quad (23)$$

for the computation of $\omega_N(Y_N, \varepsilon)$ and the computation of an ε -covering of X_N . The cost of Algorithm 3 is obtained by setting $\varepsilon = R^k r$ for $k = 0, \dots, K-1$ and summing up the resulting cost per iteration. We obtain

$$\mathcal{O}\left(\sum_{k=0}^{K-1} N_k (\log^2 N_k + (R^k r)^n N_k)\right).$$

Furthermore, exploiting the $\log(N)$ -optimality of Algorithm 2 and Equation (13) for $k \geq 1$ that

$$N_k \leq \log(N_{k-1}) \mathcal{N}(\mathcal{X}, R^{k-1} r) = \mathcal{O}((\log N_{k-1})(R^{k-1} r)^{-n}) = \mathcal{O}((\log N)(R^{k-1} r)^{-n}).$$

We arrive at

$$\begin{aligned} & \mathcal{O}\left(\sum_{k=0}^{K-1} N_k (\log^2 N_k + (R^k r)^n N_k)\right) \\ &= \mathcal{O}\left(N(\log^2 N + r^n N)\right) + \mathcal{O}\left(\sum_{k=1}^{K-1} (\log N)(R^{k-1} r)^{-n} (\log^2 N + R^n \log N)\right) \\ &= \mathcal{O}\left(N(\log^2 N + r^n N)\right) + \mathcal{O}\left((\log^3 N)r^{-n} R^{2n} \sum_{k=0}^{K-2} R^{-nk}\right) \\ &= \mathcal{O}\left(N(\log^2 N + r^n N)\right) + \mathcal{O}((\log^3 N)r^{-n} R^{n(4-K)}). \end{aligned}$$

Inserting $r = N^{-1/n}$ and $K = \lceil \log_R(T_{\mathcal{X}}/r) \rceil$ yields the assertion. \square

Based on the estimates in the proof of the previous theorem, we find the following bound on the cost of Algorithm 4.

Corollary 5.7 (Computational cost of Algorithm 4). *Assume that $(\mathcal{X}, d_{\mathcal{X}})$ is an Ahlfors n -regular metric space and let the set of data sites X_N be quasi-uniform. Then, for $R \geq 1$ and $r \approx q_{X_N} \approx N^{-1/n}$, the cost of Algorithm 4 is*

$$\begin{cases} \mathcal{O}(N(\log N + r^n N)), & t \leq r, \\ \mathcal{O}(R^{3n} r^{-n} \log^3 N), & t > r, \end{cases}$$

with constants independent of r, R , and N . Inserting $r = N^{-1/n}$, the bound becomes

$$\mathcal{O}(R^{3n} N \log^3 N) \quad \text{for all } 0 \leq t \leq T_{\mathcal{X}}.$$

Remark 5.8. *The main ingredient for the fast evaluation of the modulus of continuity using the algorithms in this section is the coarsening of the set of data sites. The proposed coarsening strategy is independent of the values of the site-to-value map. Hence, even though we will see favorable numerical experiments for Algorithm 4 in Section 8, we emphasize that the algorithm is not compliant with the consistency results in Sections 3 and 4.*

6 Piecewise constant approximation of discrete data

With a solid understanding of the discrete modulus of continuity available, we are now in the position to derive approximation results for the piecewise constant interpolation of site-to-value maps. The cost for computing such an interpolant scales linearly in the number of piecewise constant basis functions and is, for a given partition of X_N , independent of the number of data sites N .

6.1 Piecewise constant interpolation

Let a data set of the form from Equation (1) be given. To introduce piecewise constant functions on \mathcal{X} , where we may set $\mathcal{X} = X_N$ in practical applications, we introduce the partition

$$\mathcal{X} = \bigcup_{i=1}^M X^{(i)}, \quad X^{(1)}, \dots, X^{(M)} \subset \mathcal{X} \text{ mutually disjoint.}$$

For each set $X^{(i)}$, we select an interpolation point $\hat{\mathbf{x}}_i \in X^{(i)}$, $i = 1, \dots, M$, and define

$$\Xi_M := \{(\hat{\mathbf{x}}_i, X_i)\}_{i=1}^M.$$

Given a continuous function $f: \mathcal{X} \rightarrow \mathcal{Y}$, we introduce the interpolation operator

$$f \approx I_{\Xi_M} f := \sum_{i=1}^M f(\hat{\mathbf{x}}_i) \mathbb{1}_{X^{(i)}}, \quad (24)$$

where $\mathbb{1}_{X^{(i)}}$ denotes the characteristic function of the set $X^{(i)}$.

The following result is a straightforward extension of [20, Section 1.1.2].

Lemma 6.1 (Piecewise constant interpolation on compact metric spaces). *Let $f: \mathcal{X} \rightarrow \mathcal{Y}$ be of class $\rho \geq C\omega(f, \cdot)$ for some constant $C > 0$. Let $h > 0$ denote the mesh size such that $\text{diam}(X^{(i)}) \leq h$ for $i = 1, \dots, M$. Then, the interpolation error for $I_{\Xi_M} f$ from Equation (24) satisfies*

$$\sup_{\mathbf{x} \in \mathcal{X}} d_{\mathcal{Y}}(f, I_{\Xi_M} f) \leq \rho(h) |f|_{\rho}.$$

For the specific choice $\rho = \omega(f, \cdot)$, we obtain

$$\sup_{\mathbf{x} \in \mathcal{X}} d_{\mathcal{Y}}(f, I_{\Xi_M} f) \leq \omega(f, h).$$

Proof. There holds

$$\begin{aligned} |f|_{\rho} &= \sup_{t>0} (\rho(t)^{-1} \omega(f, t)) \geq \rho(h)^{-1} \omega(f, h) = \rho(h)^{-1} \sup_{\substack{\mathbf{x}, \mathbf{x}' \in \mathcal{X}: \\ d_{\mathcal{X}}(\mathbf{x}, \mathbf{x}') \leq h}} d_{\mathcal{Y}}(f(\mathbf{x}), f(\mathbf{x}')) \\ &\geq \rho(h)^{-1} \sup_{\mathbf{x} \in \mathcal{X}} d_{\mathcal{Y}}(f, I_{\Xi_M} f). \end{aligned}$$

since each $\mathbf{x} \in X^{(i)}$ satisfies $d_{\mathcal{X}}(\mathbf{x}, \mathbf{x}_i) \leq h$. Multiplying the inequality by $\rho(h)$ yields the assertion. \square

Remark 6.2. *It is easy to see that the cost of applying the interpolation operator from Equation (24) is $\mathcal{O}(M)$, independently of the cardinality of \mathcal{X} . Moreover, the approximation estimate from Lemma 6.1 is independent of the chosen interpolation points $\{\hat{\mathbf{x}}_i\}_{i=1}^M$. Thus, we may choose these points randomly within their containing sets $X^{(i)}$. This implies that the interpolation operator itself can be constructed in $\mathcal{O}(M)$, if the partition $\{X^{(i)}\}_{i=1}^M$ is already available.*

Remark 6.3. For any mesh size $h > 0$, there holds

$$\mathcal{X} \subset \bigcup_{\mathbf{x} \in \mathcal{X}} \text{int}(B_{h/2}(\mathbf{x})),$$

where $\text{int}(B_{h/2}(\mathbf{x}))$ is the interior of $B_{h/2}(\mathbf{x})$. Since \mathcal{X} is compact, we may always select M balls with corresponding centers such that

$$\mathcal{X} \subset \bigcup_{i=1,\dots,M} \text{int}(B_{h/2}(\hat{\mathbf{x}}_i)) \subset \bigcup_{i=1,\dots,M} B_{h/2}(\hat{\mathbf{x}}_i).$$

Setting

$$X^{(i)} := \left\{ \mathbf{x} \in \mathcal{X} : i = \min \left\{ k : d_{\mathcal{X}}(\hat{\mathbf{x}}_k, \mathbf{x}) = \min_{\ell=1,\dots,M} d_{\mathcal{X}}(\hat{\mathbf{x}}_{\ell}, \mathbf{x}) \right\} \right\}$$

then yields a suitable Voronoi-type partition with cell diameter $\text{diam}(X^{(i)}) \leq h$ for $i = 1, \dots, M$.

Assuming that $\hat{\mathbf{x}}_1, \dots, \hat{\mathbf{x}}_M \subset X_N$, the previous lemma yields an analogous interpolation result for site-to-value maps.

Corollary 6.4 (Piecewise constant interpolation on data sets). *Let $f_N: X_N \rightarrow Y_N$ be of class $\rho \geq C\omega(f, \cdot)$ for some $C > 0$. Assume that there exists $h > 0$ with $\text{diam}(X^{(i)}) \leq h$, $i = 1, \dots, M$. Then the interpolation error for $I_{\Xi_M} f_N$ from Equation (24) satisfies*

$$\sup_{\mathbf{x} \in \mathcal{X}} d_{\mathcal{Y}}(f_N, I_{\Xi_M} f_N) \leq \rho(h) |f_N|_{\rho, N}.$$

For the specific choice $\rho = \omega_N(f, \cdot)$ we particularly obtain

$$\sup_{\mathbf{x} \in \mathcal{X}} d_{\mathcal{Y}}(f_N, I_{\Xi_M} f_N) \leq \omega_N(f_N, h). \quad (25)$$

The upper bound based on the discrete modulus of continuity is fully discrete, compare also the definition of the discrete modulus of continuity from Equations (6) and (7). It is therefore in principle computable. For large data sets it can be estimated using the algorithms from Section 5.

Remark 6.5. *It is tempting to conjecture that a function of class ρ with $\rho \in o(t)$ as $t \rightarrow 0$ leads to a higher-order approximation. While true from an approximation theoretic perspective, these kind of function classes are rather restrictive in general. For example, it is well known that Hölder continuous functions with $\alpha > 1$, that is, $\rho(t) = t^{\alpha}$, on connected domains in \mathbb{R}^d are necessarily constant.*

Under the additional assumption that $(\mathcal{Y}, \|\cdot\|_{\mathcal{Y}})$ is a normed space, the results in Lemma 6.1 and Corollary 6.4, respectively, can be rephrased with respect to the usual sup-norm

$$\|f\|_{C(\mathcal{X}; \mathcal{Y})} := \sup_{\mathbf{x} \in \mathcal{X}} \|f(\mathbf{x})\|_{\mathcal{Y}}.$$

We further observe that the interpolation operator (24) is stable in this case, that is,

$$\|I_{\Xi_M} f\|_{C(\mathcal{X}; \mathcal{Y})} \leq \|f\|_{C(\mathcal{X}; \mathcal{Y})}. \quad (26)$$

6.2 Interpolation in Hölder spaces

If $(\mathcal{Y}, \|\cdot\|_{\mathcal{Y}})$ is a normed space, the previous approximation results relate to more conventional approximation results for Hölder continuous functions.

Corollary 6.6 (Piecewise constant interpolation in Hölder spaces). *Let \mathcal{Y} be a normed vector space. Let $f: \mathcal{X} \rightarrow \mathcal{Y}$ satisfy $|f|_{\text{Lip}(\alpha)} := |f|_{t^{\alpha}} < \infty$ for some $\alpha \in (0, 1)$. Assume that there exists a mesh size $h > 0$ with $\text{diam}(X^{(i)}) \leq h$ for $i = 1, \dots, M$. Then, there holds*

$$\|f - I_{\Xi_M} f\|_{C(\mathcal{X}; \mathcal{Y})} \leq h^{\alpha} |f|_{\text{Lip}(\alpha)}. \quad (27)$$

As before, we have an analogous result for site-to-value maps, which we state for completeness.

Corollary 6.7 (Piecewise constant interpolation in Hölder spaces on data sets). *Let \mathcal{Y} be a normed vector space. Under the assumptions of Corollary 6.4, there holds with $|f_N|_{\text{Lip}(\alpha),N} := |f_N|_{t^\alpha, N}$ that*

$$\|f_N - I_{\Xi_M} f_N\|_{C(X_N; \mathcal{Y})} \leq h^\alpha |f_N|_{\text{Lip}(\alpha),N}.$$

Remark 6.8. *Obviously, for $N < \infty$, the semi-norm $|f_N|_{\text{Lip}(\alpha),N}$ is always bounded. This implies that any site-to-value map is Hölder continuous for any Hölder exponent $\alpha \leq 1$. Hence, to distinguish between different Hölder regularity, it is suggested in [24] to introduce an explicit constant $C > 0$ and to define the discrete Hölder class of functions with $|f_N|_{\text{Lip}(\alpha),N} \leq C$. This additional assumption can be dropped, if the limit $f_N \rightarrow f$ with $|f|_{\text{Lip}(\alpha)} < \infty$ exists, see Theorems 3.12 and 4.11.*

7 Multilevel Monte Carlo for discrete data

As a relevant application for the piecewise constant approximation of discrete data, we consider the computation of first and second order statistics of independent samples of identically distributed random vectors. To this end, let $Y: \mathcal{X} \times \Omega \rightarrow \mathcal{Y}$ be a random field taking values in a real, separable Hilbert space $(\mathcal{Y}, (\cdot, \cdot)_\mathcal{Y})$, where $(\Omega, \mathcal{F}, \mathbb{Q})$ is a complete probability space. In addition, we assume that \mathcal{X} is equipped with a probability measure.

Sampling Y at certain locations $X_N = \{\mathbf{x}_1, \dots, \mathbf{x}_N\}$ amounts to a sample of random vectors

$$\mathbf{y}(\omega) = [Y(\mathbf{x}, \omega)]_{\mathbf{x} \in X_N} = Y_N(\omega) \in \mathcal{Y}^N. \quad (28)$$

Given samples $\mathbf{y}_1, \dots, \mathbf{y}_Q$ of \mathbf{y} we aim at efficiently computing the *sample mean*

$$\bar{\mathbf{y}} := \frac{1}{Q} \sum_{k=1}^Q \mathbf{y}_k, \quad (29)$$

the *sample covariance*

$$\bar{\mathbf{C}}^{(\text{Cov})} := \frac{1}{Q-1} \sum_{k=1}^Q (\mathbf{y}_k - \bar{\mathbf{y}})(\mathbf{y}_k - \bar{\mathbf{y}})^\top = \frac{1}{Q-1} \left(\mathbf{Y} \mathbf{Y}^\top - Q \bar{\mathbf{y}} \bar{\mathbf{y}}^\top \right), \quad (30)$$

and the *sample correlation*

$$\bar{\mathbf{C}}^{(\text{Cor})} := \frac{1}{Q} \sum_{k=1}^Q \mathbf{y}_k \mathbf{y}_k^\top = \frac{1}{Q} \mathbf{Y} \mathbf{Y}^\top, \quad (31)$$

with the data matrix

$$\mathbf{Y} := [\mathbf{y}_1, \dots, \mathbf{y}_Q] \in \mathcal{Y}^{N \times Q}.$$

Clearly, the sample covariance can be deduced from the sample mean and the sample correlation, such that we restrict our discussion to the latter two quantities.

Computing the sample mean (29) naively is of cost $\mathcal{O}(QN)$, while forming the product $\mathbf{Y} \mathbf{Y}^\top$ in (31) using the singular value decomposition of \mathbf{Y} is of cost $\min\{N^2Q, NQ^2\}$ and, hence, only efficient if either $Q \ll N$ or $N \ll Q$. For $Q \approx N$, (29) scales quadratically in the number of data sites, while (31) scales cubically in the number of data sites. To mitigate this cost, we assume that Y is contained pathwise in the Banach space

$$C_\rho(\mathcal{X}, \mathcal{Y}) = \{f \in C(\mathcal{X}, \mathcal{Y}): |f|_\rho < \infty\}$$

which is equipped with the norm

$$\|f\|_{C_\rho}(\mathcal{X}, \mathcal{Y}) = \|f\|_{C(\mathcal{X}, \mathcal{Y})} + |f|_\rho.$$

Similar estimates in terms of approximation and stability as in Section 6.2 can be stated. A suitable choice for ρ is the pointwise essential supremum over all pathwise moduli of continuity, that is,

$$\rho(t) = \|\omega_N(Y_N(\cdot), t)\|_{L^\infty(\Omega)}.$$

7.1 Piecewise constant approximation of empirical statistics

We assume that Y is contained in the *Lebesgue-Bochner space* $L^p(\Omega; C_\rho(\mathcal{X}; \mathcal{Y}))$, $p \geq 1$. We recall that, given a Banach space $(\mathcal{E}, \|\cdot\|_{\mathcal{E}})$, the Lebesgue-Bochner space $L^p(\Omega; \mathcal{E})$ consists of all equivalence classes of strongly \mathbb{Q} -measurable maps $f: \Omega \rightarrow \mathcal{E}$ with finite norm

$$\|f\|_{L^p(\Omega; \mathcal{E})} := \begin{cases} \left(\int_{\Omega} \|f\|_{\mathcal{E}}^p d\mathbb{Q} \right)^{\frac{1}{p}}, & p < \infty, \\ \text{ess sup}_{\omega \in \Omega} \|f\|_{\mathcal{E}}, & p = \infty. \end{cases}$$

In the following, we specifically assume that $Y \in L^2(\Omega; C_\rho(\mathcal{X}; \mathcal{Y}))$. This particularly implies that $Y \in L^2(\Omega; L^2(\mathcal{X}; \mathcal{Y}))$. Then, given an independent sample Y_1, \dots, Y_Q of Y , the sample mean

$$E_Q[Y] := \frac{1}{Q} \sum_{k=1}^Q Y_k$$

satisfies

$$\|\mathbb{E}[Y] - E_Q[Y]\|_{L^2(\Omega; L^2(\mathcal{X}; \mathcal{Y}))}^2 \leq \frac{1}{Q} \|Y\|_{L^2(\Omega; L^2(\mathcal{X}; \mathcal{Y}))}^2, \quad (32)$$

see [3] and also [40, Chapter 9]. Furthermore, it is easy to see that

$$\begin{aligned} \|Y\|_{L^2(\Omega; L^2(\mathcal{X}; \mathcal{Y}))}^2 &= \int_{\Omega} \|Y\|_{L^2(\mathcal{X}; \mathcal{Y})}^2 d\mathbb{Q} \\ &\leq \int_{\Omega} \|Y\|_{C(\mathcal{X}; \mathcal{Y})}^2 d\mathbb{Q} = \|Y\|_{L^2(\Omega; C(\mathcal{X}; \mathcal{Y}))}^2 \leq \|Y\|_{L^2(\Omega; C_\rho(\mathcal{X}; \mathcal{Y}))}^2. \end{aligned}$$

Combining the previous estimates with (32) and taking square roots yields

$$\|\mathbb{E}[Y] - E_Q[Y]\|_{L^2(\Omega; L^2(\mathcal{X}; \mathcal{Y}))} \leq \frac{1}{\sqrt{Q}} \|Y\|_{L^2(\Omega; C_\rho(\mathcal{X}; \mathcal{Y}))}. \quad (33)$$

In view of Lemma 6.1, given a partition $X^{(1)}, \dots, X^{(M)}$ with $\text{diam}(X^{(i)}) \leq h$, we can further estimate

$$\begin{aligned} &\|\mathbb{E}[Y] - E_Q[I_{\Xi_M} Y]\|_{L^2(\Omega; L^2(\mathcal{X}; \mathcal{Y}))} \\ &\leq \|\mathbb{E}[Y] - \mathbb{E}[I_{\Xi_M} Y]\|_{L^2(\Omega; L^2(\mathcal{X}; \mathcal{Y}))} + \|\mathbb{E}[I_{\Xi_M} Y] - E_Q[I_{\Xi_M} Y]\|_{L^2(\Omega; L^2(\mathcal{X}; \mathcal{Y}))} \\ &\leq \|Y - I_{\Xi_M} Y\|_{L^2(\Omega; C(\mathcal{X}; \mathcal{Y}))} + \frac{1}{\sqrt{Q}} \|I_{\Xi_M} Y\|_{L^2(\Omega; L^2(\mathcal{X}; \mathcal{Y}))} \\ &\leq \left(\rho(h) + \frac{1}{\sqrt{Q}} \right) \|Y\|_{L^2(\Omega; C_\rho(\mathcal{X}; \mathcal{Y}))} \end{aligned}$$

by invoking Bochner's inequality and the stability estimate (26).

Moreover, since $Y \in L^2(\Omega; C_\rho(\mathcal{X}; \mathcal{Y}))$, the correlation

$$\text{Cor}[Y](\mathbf{x}, \mathbf{x}') = \int_{\Omega} Y(\mathbf{x}, \omega) Y(\mathbf{x}', \omega) d\mathbb{Q}$$

exists and satisfies $\text{Cor}[Y] \in C_\rho(\mathcal{X}; \mathcal{Y}) \otimes C_\rho(\mathcal{X}; \mathcal{Y})$ for both, the injective and the projective tensor product, see [35, Chapter 3]. Similarly to the case of the expectation, we find

$$\begin{aligned} &\|\mathbb{E}[Y \otimes Y] - E_Q[I_{\Xi_M} Y \otimes I_{\Xi_M} Y]\|_{L^2(\Omega; L^2(\mathcal{X}; \mathcal{Y}) \otimes L^2(\mathcal{X}; \mathcal{Y}))} \\ &\leq \|Y \otimes Y - I_{\Xi_M} Y \otimes I_{\Xi_M} Y\|_{L^2(\Omega; C(\mathcal{X}; \mathcal{Y}))} + \frac{1}{\sqrt{Q}} \|I_{\Xi_M} Y \otimes I_{\Xi_M} Y\|_{L^2(\Omega; L^2(\mathcal{X}; \mathcal{Y}))} \\ &\leq \left(2\rho(h) + \frac{1}{\sqrt{Q}} \right) \|Y\|_{L^2(\Omega; C_\rho(\mathcal{X}; \mathcal{Y}) \otimes C_\rho(\mathcal{X}; \mathcal{Y}))} \end{aligned}$$

by standard tensor product arguments.

Fixing a set of data sites $X_N = \{\mathbf{x}_1, \dots, \mathbf{x}_N\} \subset \mathcal{X}$, the corresponding random vector $\mathbf{y}(\omega)$, see (28), satisfies

$$\mathbf{y} \in L^2(\Omega; C_\rho(X_N; \mathcal{Y})) \subset L^2(\Omega; L^2(X_N; \mathcal{Y})).$$

The previous derivation directly carries over to this case and results in the error estimates

$$\|\mathbb{E}[\mathbf{y}] - E_Q[I_{\Xi_M} \mathbf{y}]\|_{L^2(\Omega; L^2(X_N; \mathcal{Y}))} \leq \left(\rho(h) + \frac{1}{\sqrt{Q}} \right) \|\mathbf{y}\|_{L^2(\Omega; C_\rho(X_N; \mathcal{Y}))}$$

and

$$\begin{aligned} \|\mathbb{E}[\mathbf{y}\mathbf{y}^\top] - E_Q[(I_{\Xi_M} \mathbf{y})(I_{\Xi_M} \mathbf{y})^\top]\|_{L^2(\Omega; L^2(X_N; \mathcal{Y}) \otimes L^2(X_N; \mathcal{Y}))} \\ \leq \left(2\rho(h) + \frac{1}{\sqrt{Q}} \right) \|\mathbf{y}\|_{L^2(\Omega; C_\rho(X_N; \mathcal{Y}) \otimes C_\rho(X_N; \mathcal{Y}))}, \end{aligned}$$

respectively.

It is easy to see that the error is equilibrated if $\rho(h) \sim Q^{-1/2}$. Even for the regular case of Lipschitz continuous functions, that is, $\rho(t) = t$, and quasi-uniform spatial points in $\mathcal{X} = \mathbb{R}^d$, that is, $h \sim N^{-1/d}$, this implies $N \sim Q^{d/2}$ and results in a cost of $\mathcal{O}(Q^{1+d/2})$ for the computation of $E_Q[I_{\Xi_M} \mathbf{y}]$ and in a cost of $\mathcal{O}(Q^{1+d})$ for the computation of $E_Q[(I_{\Xi_M} \mathbf{y})(I_{\Xi_M} \mathbf{y})^\top]$, which is intractable. To significantly reduce this cost, we shall employ sparse tensor product techniques, that is, the multilevel Monte Carlo method for the sample mean and the multiindex Monte Carlo method for the correlation.

7.2 Multilevel Monte Carlo method

In this section, we propose a multilevel Monte Carlo approach, see [25] and the references therein, for discrete data. Given a uniform binary tree \mathcal{T} for the set $X_N \subset \mathcal{X}$, we consider the partitions

$$\Xi_j := \{(\mathbf{x}_\tau, \tau) : \tau \in \mathcal{T}, \ell(\tau) = j\}, \quad \text{for } j = 0, \dots, J,$$

where the interpolation points $\mathbf{x}_\tau \in \tau$ may be chosen arbitrarily. A nested sequence of interpolation points can be obtained by the choice $\mathbf{x}_\tau \in \{\mathbf{x}_{\tau'} : \tau' \in \text{children}(\tau)\}$ for $\tau \in \mathcal{T} \setminus \mathcal{L}$.

We have the following lemma, which bounds the pointwise difference of two consecutive interpolants. The result directly carries over to site-to-value maps in $C_\rho(X_N; \mathcal{Y})$.

Lemma 7.1. *There holds for any $f \in C_\rho(\mathcal{X}; \mathcal{Y})$ that*

$$\|I_{\Xi_j} f - I_{\Xi_{j-1}} f\|_{C(\mathcal{X}; \mathcal{Y})} \leq 2\rho(c_{\text{diam}} 2^{-c_{\text{uni}}(j-1)}) \|f\|_{C_\rho(\mathcal{X}; \mathcal{Y})}, \quad (34)$$

where the constants $c_{\text{diam}}, c_{\text{uni}} > 0$ depend on the uniformity from Definition 5.4.

Proof. By the triangle inequality, we have

$$\begin{aligned} \|I_{\Xi_j} f - I_{\Xi_{j-1}} f\|_{C(\mathcal{X}; \mathcal{Y})} &\leq \|I_{\Xi_j} f - f\|_{C(\mathcal{X}; \mathcal{Y})} + \|I_{\Xi_{j-1}} f - f\|_{C(\mathcal{X}; \mathcal{Y})} \\ &\leq \left(\rho(c_{\text{diam}} 2^{-c_{\text{uni}}j}) + \rho(c_{\text{diam}} 2^{-c_{\text{uni}}(j-1)}) \right) \|f\|_{C_\rho(\mathcal{X}; \mathcal{Y})} \\ &\leq 2\rho(c_{\text{diam}} 2^{-c_{\text{uni}}(j-1)}) \|f\|_{C_\rho(\mathcal{X}; \mathcal{Y})} \end{aligned}$$

due to $\text{diam}(\tau) \leq c_{\text{diam}} 2^{-c_{\text{uni}}j}$ and using Lemma 6.1. \square

The decay across scales, shown in the previous lemma, corresponds to a level-wise variance reduction in case of random fields. This stipulates the idea of the multilevel Monte Carlo estimator. Given a sequence $Q_0 \geq \dots \geq Q_J$ of natural numbers, the multilevel Monte Carlo estimator reads

$$E^{\text{ML}}[Y] := \sum_{j=0}^J E_{Q_{J-j}}[(I_{\Xi_j} - I_{\Xi_{j-1}})Y], \quad \text{where } I_{\Xi_{-1}} Y \equiv 0.$$

The following theorem is a well established result on the multilevel Monte Carlo estimator. We provide its proof here adapted to the present context for the readers convenience.

Theorem 7.2. Let $Y \in L^2(\Omega; C_\rho(\mathcal{X}; \mathcal{Y}))$. Then there holds

$$\|\mathbb{E}[Y] - E^{\text{ML}}[Y]\|_{L^2(\Omega; L^2(\mathcal{X}; \mathcal{Y}))} \leq \sigma_{\text{ML}}(J, \rho, \{Q_j\}_j) \|Y\|_{L^2(\Omega; C_\rho(\mathcal{X}; \mathcal{Y}))}$$

with the convergence factor

$$\sigma_{\text{ML}}(J, \rho, \{Q_j\}_j) := \rho(c_{\text{diam}} 2^{-c_{\text{uni}} J}) + 2 \sum_{j=0}^J \frac{\rho(c_{\text{diam}} 2^{-c_{\text{uni}}(j-1)})}{\sqrt{Q_{J-j}}}. \quad (35)$$

Proof. By the triangle inequality, we obtain

$$\begin{aligned} & \|\mathbb{E}[Y] - E^{\text{ML}}[Y]\|_{L^2(\Omega; L^2(\mathcal{X}; \mathcal{Y}))} \\ & \leq \|\mathbb{E}[Y] - \mathbb{E}[I_{\Xi_J} Y]\|_{L^2(\Omega; L^2(\mathcal{X}; \mathcal{Y}))} + \|\mathbb{E}[I_{\Xi_J} Y] - E^{\text{ML}}[Y]\|_{L^2(\Omega; L^2(\mathcal{X}; \mathcal{Y}))}. \end{aligned}$$

The first term on the left-hand side can be estimated by Lemma 6.1 and Bochner's inequality. For the second term, we obtain by the linearity of expectation, the fact that $I_{\Xi_J} Y = \sum_{j=0}^J (I_{\Xi_j} - I_{\Xi_{j-1}}) Y$ and the triangle inequality that

$$\begin{aligned} & \|\mathbb{E}[I_{\Xi_J} Y] - E^{\text{ML}}[Y]\|_{L^2(\Omega; L^2(\mathcal{X}; \mathcal{Y}))} \\ & = \left\| \sum_{j=0}^J \mathbb{E}[(I_{\Xi_j} - I_{\Xi_{j-1}}) Y] - E_{Q_{J-j}}[(I_{\Xi_j} - I_{\Xi_{j-1}}) Y] \right\|_{L^2(\Omega; L^2(\mathcal{X}; \mathcal{Y}))} \\ & \leq \sum_{j=0}^J \|\mathbb{E}[(I_{\Xi_j} - I_{\Xi_{j-1}}) Y] - E_{Q_{J-j}}[(I_{\Xi_j} - I_{\Xi_{j-1}}) Y]\|_{L^2(\Omega; L^2(\mathcal{X}; \mathcal{Y}))}. \end{aligned}$$

Employing Equations (32) and (34), we obtain for the terms within the sum that

$$\begin{aligned} & \|\mathbb{E}[(I_{\Xi_j} - I_{\Xi_{j-1}}) Y] - E_{Q_{J-j}}[(I_{\Xi_j} - I_{\Xi_{j-1}}) Y]\|_{L^2(\Omega; L^2(\mathcal{X}; \mathcal{Y}))} \\ & \leq \frac{1}{\sqrt{Q_{J-j}}} \|I_{\Xi_j} Y - I_{\Xi_{j-1}} Y\|_{L^2(\Omega; L^2(\mathcal{X}; \mathcal{Y}))} \leq 2 \frac{\rho(c_{\text{diam}} 2^{-c_{\text{uni}}(j-1)})}{\sqrt{Q_{J-j}}} \|Y\|_{L^2(\Omega; C_\rho(\mathcal{X}; \mathcal{Y}))}. \end{aligned}$$

Combining the preceding estimates, we finally arrive at the error bound

$$\|\mathbb{E}[I_{\Xi_J} Y] - E^{\text{ML}}[Y]\|_{L^2(\Omega; L^2(D))} \leq \left(\rho(c_{\text{diam}} 2^{-c_{\text{uni}} J}) + 2 \sum_{j=0}^J \frac{\rho(c_{\text{diam}} 2^{-c_{\text{uni}}(j-1)})}{\sqrt{Q_{J-j}}} \right) \|Y\|_{L^2(\Omega; C_\rho(\mathcal{X}; \mathcal{Y}))}.$$

□

In principle, a similar estimator with similar error bound could also be stated for the correlation. However, the computational cost of the arising estimator will be dominated by the quadratic cost of assembling the samples $I_{\Xi_k} Y \otimes I_{\Xi_k} Y$. Instead, we observe that applying (34) to two different levels of a dyad $f \otimes f \in C_\rho(\mathcal{X}; \mathcal{Y}) \otimes C_\rho(\mathcal{X}; \mathcal{Y})$ results in the bound

$$\begin{aligned} & \|(I_{\Xi_j} - I_{\Xi_{j-1}}) f \otimes (I_{\Xi'_j} - I_{\Xi'_{j-1}}) f\|_{C(\mathcal{X}; \mathcal{Y}) \otimes C(\mathcal{X}; \mathcal{Y})} \\ & \leq 4 \rho(c_{\text{diam}} 2^{-c_{\text{uni}}(j-1)}) \rho(c_{\text{diam}} 2^{-c_{\text{uni}}(j'-1)}) \|f \otimes f\|_{C_\rho(\mathcal{X}; \mathcal{Y}) \otimes C_\rho(\mathcal{X}; \mathcal{Y})}. \end{aligned} \quad (36)$$

This suggests the multiindex or sparse tensor product estimator

$$E^{\text{MI}}[Y \otimes Y] := \sum_{j=0}^J \sum_{k+k'=j} E_{Q_{J-j}}[(I_{\Xi_k} - I_{\Xi_{k-1}}) Y \otimes (I_{\Xi'_{k'}} - I_{\Xi'_{k'-1}}) Y]$$

for the sample correlation. The important difference to the multilevel estimator is that the tensor products are formed between interpolants at different levels, which reduces the computational footprint. In analogy to Theorem 7.2, we obtain the following result.

Theorem 7.3. Let $Y \in L^2(\Omega; C_\rho(\mathcal{X}; \mathcal{Y}))$. Then, there holds

$$\|\mathbb{E}[Y \otimes Y] - E^{\text{MI}}[Y \otimes Y]\|_{L^2(\Omega; L^2(\mathcal{X}; \mathcal{Y}) \otimes L^2(\mathcal{X}; \mathcal{Y}))} \leq \sigma_{\text{MI}}(J, \rho, \{Q_j\}_j) \|Y \otimes Y\|_{L^2(\Omega; C_\rho(\mathcal{X}; \mathcal{Y}) \otimes C_\rho(\mathcal{X}; \mathcal{Y}))}$$

with the convergence factor

$$\sigma_{\text{MI}}(J, \rho, \{Q_j\}_j) := 2\rho(c_{\text{diam}} 2^{-c_{\text{uni}} J}) + 4 \sum_{j=0}^J \sum_{k+k'=j} \frac{\rho(c_{\text{diam}} 2^{-c_{\text{uni}}(k-1)}) \rho(c_{\text{diam}} 2^{-c_{\text{uni}}(k'-1)})}{\sqrt{Q_{J-j}}}. \quad (37)$$

Replacing Y in Theorems 7.2 and 7.3 by its discrete version \mathbf{y} immediately yields the following corollary.

Corollary 7.4. Let $\mathbf{y} \in L^2(\Omega; C_\rho(X_N; \mathcal{Y}))$. Then, there holds

$$\|\mathbb{E}[\mathbf{y}] - E^{\text{ML}}[\mathbf{y}]\|_{L^2(\Omega; L^2(X_N; \mathcal{Y}))} \leq \sigma_{\text{ML}}(J, \rho, \{Q_j\}_j) \|\mathbf{y}\|_{L^2(\Omega; C_\rho(X_N; \mathcal{Y}))}$$

and

$$\|\mathbb{E}[\mathbf{y}\mathbf{y}^\top] - E^{\text{MI}}[\mathbf{y}\mathbf{y}^\top]\|_{L^2(\Omega; L^2(X_N; \mathcal{Y}) \otimes L^2(X_N; \mathcal{Y}))} \leq \sigma_{\text{MI}}(J, \rho, \{Q_j\}_j) \|\mathbf{y}\mathbf{y}^\top\|_{L^2(\Omega; C_\rho(X_N; \mathcal{Y}) \otimes C_\rho(X_N; \mathcal{Y}))}.$$

respectively.

Assuming additional structure on ρ allows for more concrete error estimates and for bounds of the computational cost of the estimators.

7.3 The multilevel Monte Carlo method for Hölder continuous functions

Our initial observation is that for Hölder continuous functions with Hölder exponent $\alpha \in (0, 1]$, the error estimate Theorem 7.2 coincides to what is known from literature. In particular, the convergence factor (35) for the multilevel Monte Carlo simplifies towards

$$\sigma_{\text{ML}}(J, t^\alpha, \{Q_j\}_j) = c_{\text{diam}}^\alpha \left(2^{-\alpha c_{\text{uni}} J} + 2^{\alpha c_{\text{uni}} + 1} \sum_{j=0}^J \frac{2^{-\alpha c_{\text{uni}} j}}{\sqrt{Q_{J-j}}} \right).$$

Based on the cost analysis from [25], in order to achieve an overall root mean square error of $1/\sqrt{Q}$, there holds for the cost C_{MLMC} of the multilevel Monte Carlo estimator that

$$C_{\text{MLMC}} = \begin{cases} \mathcal{O}(Q), & \text{if } c_{\text{uni}}\alpha > 1, \\ \mathcal{O}(Q \log^2 Q), & \text{if } c_{\text{uni}}\alpha = 1, \\ \mathcal{O}(Q^{\frac{1}{2} + \frac{1}{2c_{\text{uni}}\alpha}}), & \text{if } c_{\text{uni}}\alpha < 1. \end{cases}$$

For the convergence factor (37) of the multiindex estimator, we first note that $|\{k + k' = j : k, k' \in \mathbb{N}\}| = j + 1$ is the number of weak integer compositions of j . Therefore, the convergence factor of the multiindex estimator simplifies towards

$$\sigma_{\text{MI}}(J, t^\alpha, \{Q_j\}_j) = 2^{-\alpha c_{\text{uni}} J + 1} c_{\text{diam}}^\alpha + 4^{\alpha c_{\text{uni}} + 1} c_{\text{diam}}^{2\alpha} \sum_{j=0}^J \frac{(j+1)2^{-\alpha c_{\text{uni}} j}}{\sqrt{Q_{J-j}}}.$$

Remark 7.5. Instead of using the cost bound for the multiindex estimator from [25], we may in our particular setting just use a similar cost bound as for the multilevel estimator by noticing that there exists for every $\varepsilon > 0$ a j_0 such that $(j+1) \leq 2^{\varepsilon j}$ for all $j \geq j_0$. In order to achieve an overall root mean error of $1/\sqrt{Q}$, we obtain the cost bound

$$C_{\text{MIMC}} = \begin{cases} \mathcal{O}(Q), & \text{if } c_{\text{uni}}\alpha - \varepsilon > 1, \\ \mathcal{O}(Q \log^2 Q), & \text{if } c_{\text{uni}}\alpha - \varepsilon = 1, \\ \mathcal{O}(Q^{\frac{1}{2} + \frac{1}{2(c_{\text{uni}}\alpha - \varepsilon)}}), & \text{if } c_{\text{uni}}\alpha - \varepsilon < 1. \end{cases}$$

Replacing Y by its discrete version \mathbf{y} and employing the representation of the convergence factors for the Hölder case immediately yields the following variant of Corollary 7.4.

Corollary 7.6. *Let $\mathbf{y} \in L^2(\Omega; C^{0,\alpha}(X_N; \mathcal{Y}))$. Then, there exists a constant $c_{\text{ML}} > 0$ such that*

$$\|\mathbb{E}[\mathbf{y}] - E^{\text{ML}}[\mathbf{y}]\|_{L^2(\Omega; L^2(X_N; \mathcal{Y}))} \leq c_{\text{ML}} \left(\sum_{j=0}^J \frac{2^{-c_{\text{uni}} j \alpha}}{\sqrt{Q_{J-j}}} \right) \|\mathbf{y}\|_{L^2(\Omega; C^{0,\alpha}(X_N; \mathcal{Y}))}.$$

Similarly, there exists a constant $c_{\text{MI}} > 0$ such that

$$\begin{aligned} & \|\mathbb{E}[\mathbf{y}\mathbf{y}^\top] - E^{\text{MI}}[\mathbf{y}\mathbf{y}^\top]\|_{L^2(\Omega; L^2(X_N; \mathcal{Y}) \otimes L^2(X_N; \mathcal{Y}))} \\ & \leq c_{\text{MI}} \sum_{j=0}^J \frac{(j+1)2^{-c_{\text{uni}} j \alpha}}{\sqrt{Q_{J-j}}} \|\mathbf{y}\mathbf{y}^\top\|_{L^2(\Omega; C^{0,\alpha}(X_N; \mathcal{Y}) \otimes C^{0,\alpha}(X_N; \mathcal{Y}))}. \end{aligned}$$

respectively.

We note that similar multilevel estimates as in Theorem 7.3 and Corollary 7.6 have been shown for an \mathcal{H}^2 -matrix based approach in [21] and for a wavelet based approach in [28]. Both approaches are able to approximate the second moment with optimal cost, but have limited applicability. The \mathcal{H}^2 -matrix approach is based on additional assumptions on the regularity of the second moment, which are hard to verify for general site-to-value maps. The wavelet based approach leverages the multilevel structure of wavelet representations of site-to-value maps. However, as wavelet constructions are usually confined to intervals or tensor products thereof, it remains to be investigated how the approach can be applied to general site-to-value maps.

8 Numerical examples

In this section, we verify the theoretical findings and give illustrative examples, ranging from the computation of the discrete modulus of continuity for different types of functions over the convergence of the discrete modulus of continuity and the piecewise constant approximation of discrete data to the multilevel Monte Carlo method for discrete data.

8.1 Computation of the discrete modulus of continuity

Wiener process on $[0, 1]$. In this example, we consider the pathwise smoothness of the Wiener process, that is, a Gaussian process with mean zero and covariance function $k(s, t) = \min\{s, t\}$ on $[0, 1]$. It is well known that the paths of the Wiener process are Hölder continuous for all exponents $\alpha < 1/2$. Especially, their modulus of continuity is well approximated for small t by

$$\omega(f, t) \approx \sqrt{2t \log(1/t)}. \quad (38)$$

We compute the discrete modulus of continuity using Algorithms 3 and 4, respectively for 10 different realizations of the Wiener process, where we set $r = 10^{-5}$, $R = 2$, $T = 1$. For the generation of the evaluation points of the Wiener process, we consider independently drawn uniformly distributed random numbers in $[0, 1]$. We keep these time points fixed over all runs. We employ $N = 10^6$ time points resulting in a fill distance of $h_{X_N} = 6.00 \cdot 10^{-5}$ and a separation distance of $q_{X_N} = 5.00 \cdot 10^{-12}$. To evaluate the discrete modulus of continuity by means of Algorithm 4, we choose a quadratically graded mesh with 1000 points with the smallest value being 10^{-5} and the largest value being 1.

The left panel of Figure 3 shows four realizations of the resulting discrete moduli of continuity together with the approximate analytical rate from (38), while the right panel shows the expected modulus of continuity averaged over the ten runs, where the gray shaded area corresponds to one standard deviation. As can be seen and as expected, the obtained trajectories as well as the mean closely follow the graph of (38) for small values of t .

Continuous but not Hölder continuous function on \mathbb{S}^2 . The next example is dedicated to showing that the modulus of continuity can quantify smoothness which is weaker than Hölder continuity. As an example of a continuous but not Hölder continuous function, we consider the function $f: \mathbb{S}^2 \rightarrow \mathbb{R}$ defined by

$$f(\mathbf{x}) = \begin{cases} \left| \log \frac{d_{\mathbb{S}^2}(\mathbf{x}, \mathbf{x}_0)}{\pi} - 2 \right|^{-1}, & \mathbf{x} \neq \mathbf{x}_0, \\ 0, & \mathbf{x} = \mathbf{x}_0, \end{cases} \quad (39)$$

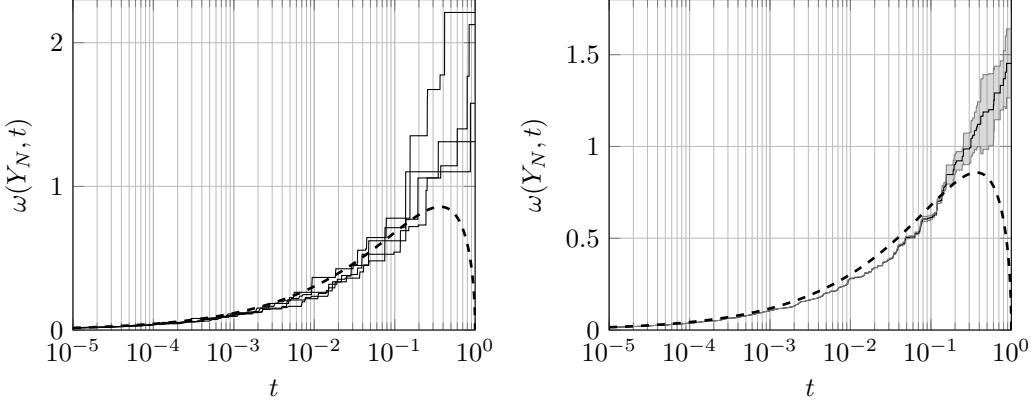


Figure 3: Samples of the discrete modulus of continuity of the Wiener process (left). Average modulus of continuity and one standard deviation envelope (right). Dashed lines indicate the approximation (38) for small t .

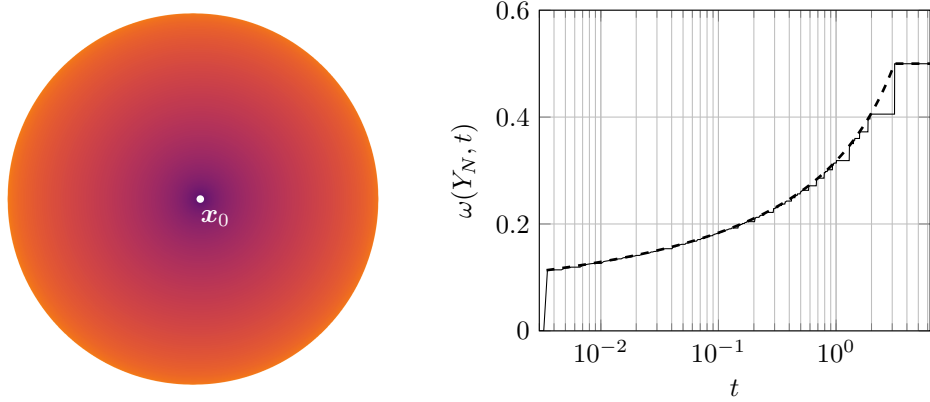


Figure 4: Continuous but not Hölder continuous function from Equation (39) on \mathbb{S}^2 (left) and corresponding discrete modulus of continuity (right). The dashed line indicates the exact modulus of continuity.

where $\mathbf{x}_0 \in \mathbb{S}^2$ and $d_{\mathbb{S}^2}(\mathbf{x}, \mathbf{y})$ denotes the geodesic distance. A visualization of this function is shown on the left hand side of Figure 4 for the choice $\mathbf{x}_0 = [1.00, 3.53 \cdot 10^{-2}, 1.00 \cdot 10^{-6}]^\top$. The function is evaluated at a Fibonacci lattice, see [43], with $N = 10^6$ points. The fill distance is $h_{X_N} \approx 3.55 \cdot 10^{-3}$ and the separation distance $q_{X_N} \approx 3.01 \cdot 10^{-3}$. Both quantities have been approximated using Euclidean distances. It is a short computation to check that the modulus of continuity of Equation (39) is given by

$$\omega(f, t) = \begin{cases} 0, & t = 0, \\ \left| \log \frac{t}{\pi} - 2 \right|^{-1}, & t \in (0, \pi), \\ \frac{1}{2}, & t \geq \pi. \end{cases} \quad (40)$$

We approximate the modulus of continuity choosing $r = 10^{-3}$, $R = 2$, $T = 2\pi$ in Algorithms 3 and 4. Within the algorithms, the distances are chosen as the geodesic distances on the sphere. The resulting approximation to the discrete modulus of continuity is found on the right hand side of Figure 4. As can be seen, the approximation closely follows the true behavior, where we notice that the discrete modulus of continuity becomes zero for $t < q_X$, as it is to be expected.

Real-world weather data Our final example concerning the estimation of the modulus of continuity considers a time series of real-world data. We consider the temperature two meters above ground level at the airport Cologne/Bonn (CGN) in $^{\circ}\text{C}$. The data is provided in 10 minute intervals by the DWD Climate Data Center (CDC) for the period from 2 December 2008 to 11

date and time (YYYY-MM-DD hh:mm:ss)	°C
⋮	⋮
2017-07-19 13:30:00	30.5
2017-07-19 13:40:00	29.6
2017-07-19 13:50:00	19.2
2017-07-19 14:00:00	18.9
⋮	⋮
2018-08-09 12:30:00	30
2018-08-09 12:40:00	29.6
2018-08-09 12:50:00	19.3
2018-08-09 13:00:00	21.2
⋮	⋮

Table 1: Excerpt from the real world weather data indicating the temperature drops responsible for the irregularity of the temperature measurements as determined by the modulus of continuity in Figure 5.

September 2025, see [9], and consists of 881 528 data points covering a time span of almost $9 \cdot 10^6$ minutes. We compute the modulus of continuity on the full data set using $r = 10$, $R = 2$, $T = 10^6$ in Algorithms 3 and 4. A daily subsample of the data set can be found on the left-hand side of

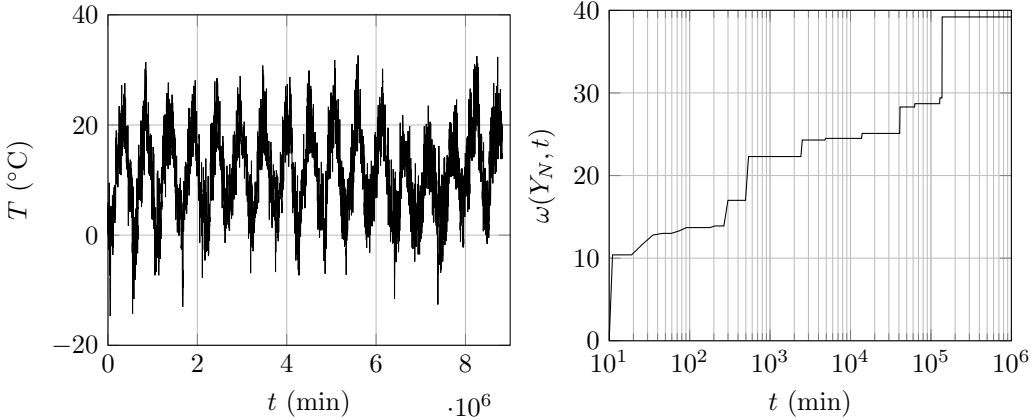


Figure 5: Time series of the real-world weather data (left) and its discrete modulus of continuity (right).

Figure 5. The separation distance is $q_{X_N} = 10$, implying that the discrete modulus of continuity is zero for $t < q_X$. The fill distance is $h_{X_N} = 60$, indicating that the dataset contains gaps with only one measurement recorded per hour. The approximate discrete modulus of continuity is shown on the right hand side of Figure 5. The modulus of continuity indicates a rather irregular behavior already at the smallest time interval of 10 minutes. Indeed, closer investigation of the data reveals several sudden temperature drops of more than 10°C within a 10 minute span, which are responsible for this irregularity, see Table 1. Thus, the modulus of continuity correctly captures the smoothness of the data.

8.2 Consistency for deterministic data sites

Consistency in L^2 We verify the consistency estimates from Corollary 3.11 in L^p for $p = 2$. To this end, we consider two test cases, namely the function $f(x) = \sqrt{x}$ on $[0, 1]$ and the univariate version of the non-Hölder continuous function from (39), that is,

$$f(x) = \begin{cases} |\log x - 2|^{-1}, & x \neq 0, \\ 0, & x = 0, \end{cases}$$

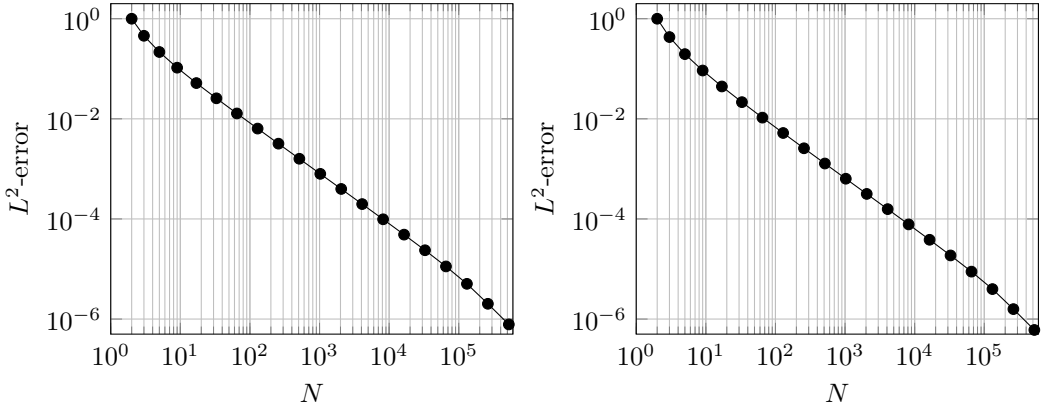


Figure 6: Convergence of the discrete modulus of continuity in L^2 for $N \rightarrow \infty$ using deterministic data sites. The left panel shows the convergence for the square root function, while the right panel shows the convergence for the log function on the interval.

also evaluated on $[0, 1]$. For the square root, the modulus of continuity is $\omega(f, t) = t^{-1/2}$, while it is

$$\omega(f, t) = \begin{cases} 0, & t = 0, \\ |\log t - 2|^{-1}, & t \in (0, 1), \\ \frac{1}{2}, & t \geq 1. \end{cases}$$

for the non-Hölder continuous function from Equation (39), see also Equation (40). To demonstrate the consistency, we compute the modulus of continuity using a brute-force approach with runtime $\mathcal{O}(N^2)$ and compare it to the true one. For the spatial discretization, we employ uniform subdivisions of the unit interval with $N = 2^j + 1$ points for $j = 0, \dots, 19$. As the discrete moduli of continuity are nonsmooth, we use a composite trapezoidal rule on $[0, 1]$ with 10^6 quadratically graded points. The resulting quadrature error is around $2.5 \cdot 10^{-13}$ for both moduli of continuity. We remark that such a high accuracy of the quadrature has been necessary, as otherwise the convergence stalled. The results are depicted in Figure 6. The left-hand side of the figure shows the convergence for the modulus of continuity of the square root, while the right-hand side shows the convergence for the modulus of continuity of the non-Hölder continuous function. As can be inferred from the figure, in both cases, the rate of convergence is approximately linear.

8.3 Consistency for empirical data sites

To show consistency also for the case of empirical data sites, we perform a similar experiment as in the previous paragraph. This time, we randomize the locations of the data sites using independently drawn uniform random points in $[0, 1]$. All other parameters are kept as before. We show the average error over 10 runs in Figure 7. As we can see from the left panel, the rate of convergence is approximately $\mathcal{O}(N^{-1/2})$ for the modulus of continuity of the square root, while it is significantly reduced for the modulus of continuity of the non-Hölder continuous function.

8.4 Piecewise constant approximation of discrete data

In this example, we verify the approximation rates for piecewise constant approximation spaces defined directly at the data sites, compare Section 6. We focus on the approximation estimate Equation (25) from Corollary 6.4 which bounds the interpolation error on data sets in terms of the discrete modulus of continuity. To this end, we use the data sets from Section 8.1 as ground truth on which we build coarser piecewise constant approximation spaces by an s - d -tree based coarsening procedure. The interpolation points for the constant approximation within the resulting clusters are chosen randomly. If a cluster at a certain level is empty, we replace its value by that of the parent. For the Wiener process, we choose $N = 10^6$ for the ground truth and set $r = 10^{-5}$, $R = 2$, $T = 1$ for the computation of the discrete modulus of continuity by Algorithms 3 and 4. As before, the time points are sampled uniformly at random from the interval $[0, 1]$ and remain fixed across ten runs. Each run selects different interpolation points and samples

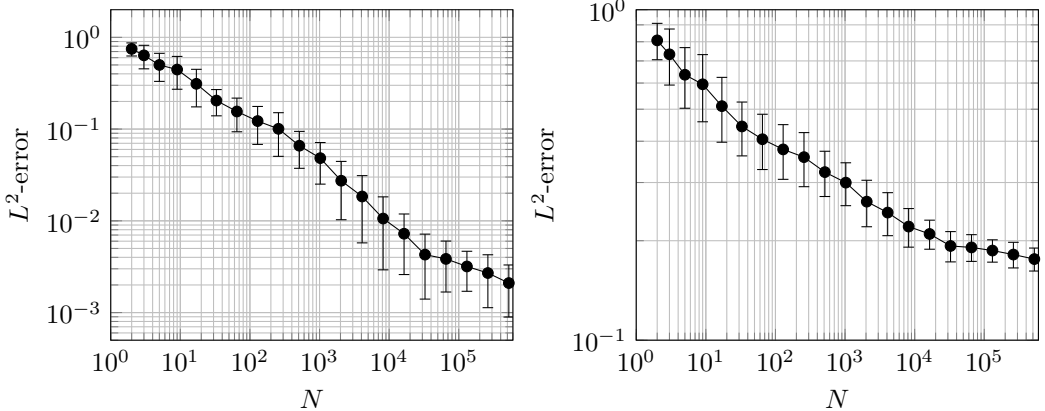


Figure 7: Convergence of the discrete modulus of continuity in L^2 for $N \rightarrow \infty$ using uniformly random data sites. The left panel shows the convergence for the square root function, while the right panel shows the convergence for the log function on the interval. The error bars correspond to one standard deviation.

a new path of the Wiener process. Figure 8 shows the average maximum pointwise approximation error versus the mesh size h , that is, the maximum cluster diameter at each level. The error

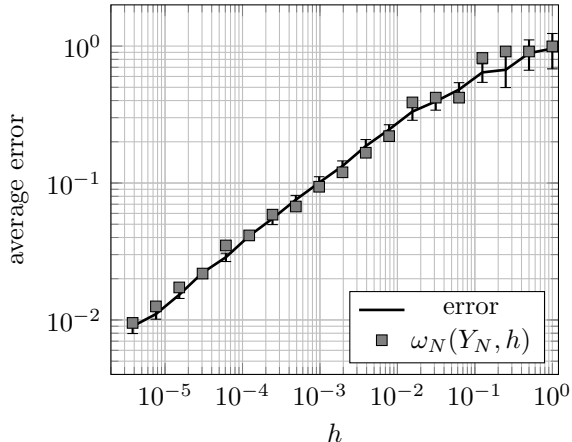


Figure 8: Average approximation error for the Wiener process on $[0, 1]$ versus the mesh size h . The error bars show one standard deviation. The gray boxes indicate the corresponding discrete modulus of continuity, evaluated approximately using Algorithms 3 and 4.

bars correspond to one standard deviation. The boxes mark the approximate discrete modulus of continuity computed for the ground truth. Especially, for smaller mesh sizes, the interpolation error is bounded by the approximate discrete modulus of continuity, as expected. For larger mesh sizes, the discrete modulus of continuity is evaluated at larger values of t , where we need to expect a larger approximation error from Algorithms 3 and 4. Still, the values of the discrete modulus of continuity are close to the true errors.

For the non-Hölder continuous function (39), we choose a Fibonacci lattice with $N = 10^6$ points as ground truth and set $r = 10^{-2}$, $R = 2$, $T = 2\pi$ for the computation of the discrete modulus of continuity by Algorithms 3 and 4. As before, the interpolation points are randomly sampled within each cluster. Figure 9 shows the average maximum pointwise approximation error versus the mesh size h , computed using ten runs. Here, the mesh size is computed using the geodesic distance. In this example, the maximum interpolation error stays clearly below the approximate discrete modulus of continuity computed for the ground truth.

Finally, we consider the entire time series data set with $N = 881528$ points and set $r = 10$, $R = 2$, $T = 10^6$ for the computation of the discrete modulus of continuity by Algorithms 3 and 4. As in the other two examples, the interpolation points are randomly sampled within each

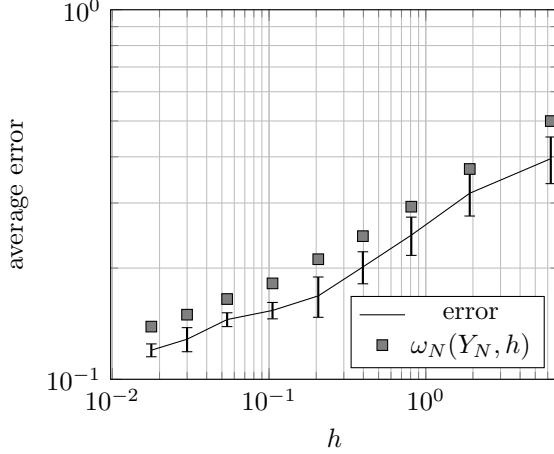


Figure 9: Average approximation error for the non-Hölder continuous function (39) on \mathbb{S}^2 versus the mesh size h . The error bars show one standard deviation. The gray boxes indicate the corresponding discrete modulus of continuity, evaluated approximately using Algorithms 3 and 4.

cluster. Figure 10 shows the average maximum pointwise approximation error versus the mesh size h , computed using ten runs. Here, for the large and the small values of the mesh size, the

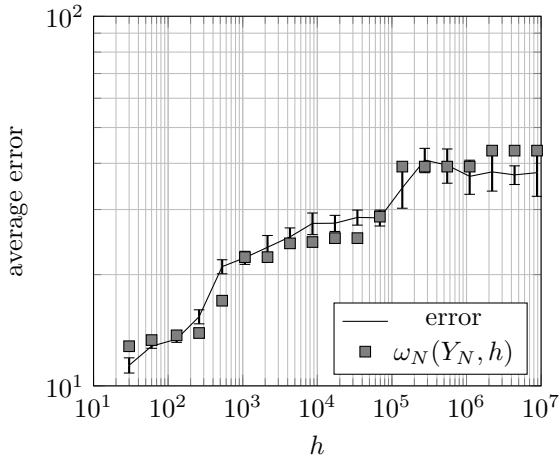


Figure 10: Average approximation error for the time series data versus the mesh size h . The error bars show one standard deviation. The gray boxes indicate the corresponding approximate discrete modulus of continuity, evaluated approximately using Algorithms 3 and 4.

discrete modulus of continuity bounds the approximation error, while it is slightly smaller than the approximation error for intermediate mesh sizes. We attribute this again to the approximation error of Algorithms 3 and 4.

8.5 Multilevel Monte Carlo

Wiener process In this example, we consider the multilevel Monte Carlo approximation of the mean of the Wiener process on $[0, 1]$, sampled at random time points as in Section 8.1. Four different realizations of the Wiener process are depicted in Figure 11.

As noted before, the paths of the Wiener process are Hölder continuous for all exponents $\alpha < 1/2$. Hence, in view of Corollary 6.6, based on a balanced binary tree, the variance at level ℓ scales as $V_\ell = \mathcal{O}(2^{-\alpha\ell})$, while the cost is linear with the level, that is, $C_\ell = \mathcal{O}(2^\ell)$. Therefore, the number of samples to achieve an overall root mean square error of $1/\sqrt{N}$ has to scale like $\sqrt{V_\ell}/C_\ell$ on level ℓ , see [25]. Consequently, choosing $N_0 = N$ samples at the coarsest level, the number of

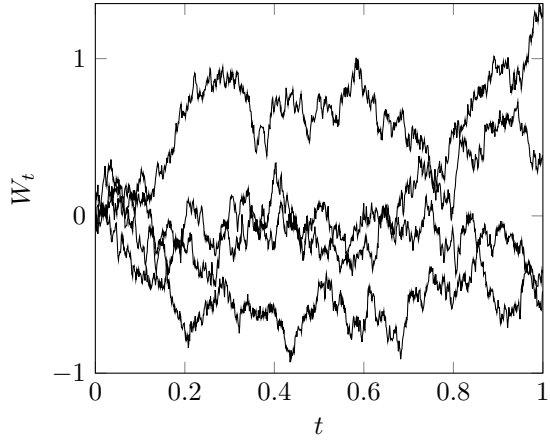


Figure 11: Different realizations of the Wiener process on $[0, 1]$.

samples has to decrease by a factor of $N_\ell/N_{\ell-1} = \sqrt{V_\ell/V_{\ell-1}} \cdot \sqrt{C_{\ell-1}/C_\ell}$. In the current example this leads to $N_\ell/N_{\ell-1} = 2^{-(\alpha+1)/2} \approx 2^{-3/2}$.

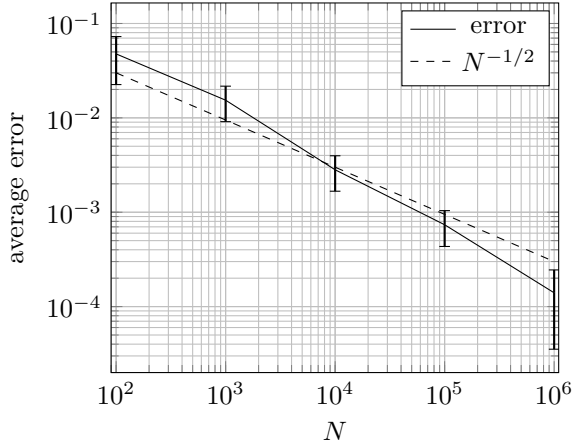


Figure 12: Average error of the multilevel Monte Carlo approximation of the mean of the Wiener process for different N over ten different runs. The error bars show one standard deviation.

The convergence of the multilevel Monte Carlo approximation to the mean of the Wiener process on $[0, 1]$ is shown in Figure 12. The figure shows the maximum error averaged over 10 runs. The error bars indicate one standard deviation. Over each of these runs, the uniform random timepoints points for the Wiener process are kept fixed, while the interpolation points used for the multilevel Monte Carlo method are randomized in each leaf of the cluster tree. Nested interpolation points are obtained by selecting the first non-empty child and assigning its sample point to the parent cluster. This interpolation procedure is compliant with the theoretical result in Corollary 6.6. The theoretical rate of $N^{-1/2}$ is clearly achieved in this example.

Isotropic Gaussian random field on \mathbb{S}^2 . We consider an isotropic Gaussian field on the unit sphere \mathbb{S}^2 with mean zero and covariance function $k(\mathbf{x}, \mathbf{y}) = e^{-4d_{\mathbb{S}^2}(\mathbf{x}, \mathbf{y})}$, where $d_{\mathbb{S}^2}(\mathbf{x}, \mathbf{y})$ denotes the geodesic distance. The field is evaluated at a Fibonacci lattice. Figure 13 shows the resulting points for $N = 10^2, 10^3, 10^4, 10^5$ together with the bounding boxes of the leaves of the corresponding s -d-tree.

Since the paths of the field are only Hölder continuous with coefficient $\alpha < 1/2$, they cannot efficiently be approximated by a spectral approach. Therefore, we perform the sampling using a Krylov subspace approximation of the matrix square root. For $N \leq 10^3$, we directly use the covariance matrix, while for larger N , we first perform a sample matrix compression thereof, see [29] and the references therein. We use samplets with three vanishing moments and the cutoff

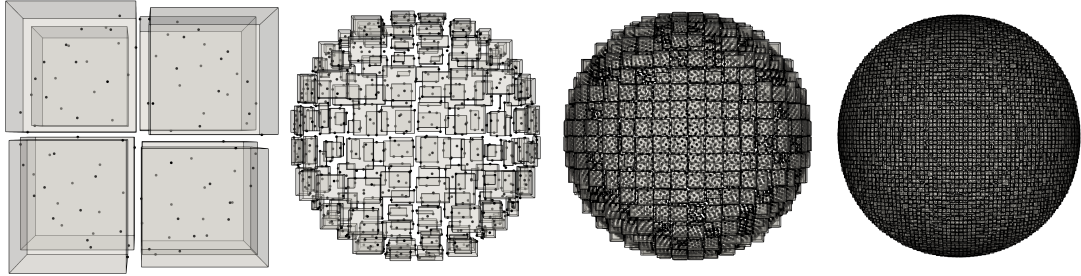


Figure 13: Fibonacci lattices for the unit sphere with 10^2 , 10^3 , 10^4 , 10^5 points and bounding boxes of the leaves of the corresponding s -d-trees.

criterion is set to $\eta = 10$. An a-posteriori compression is performed with a relative threshold of 10^{-4} in the Frobenius norm. For $N = 10^6$, the resulting compression error is $1.53 \cdot 10^{-4}$ using a randomized estimator. The compressed matrix contains 141 entries per row on average. For all N , we employ a Krylov subspace of dimension 10. Four different realizations of the computed Gaussian field can be found in Figure 14. Particularly, we observe that the high frequency oscillations in the realizations, known from the Wiener process, are captured by the taken approach.

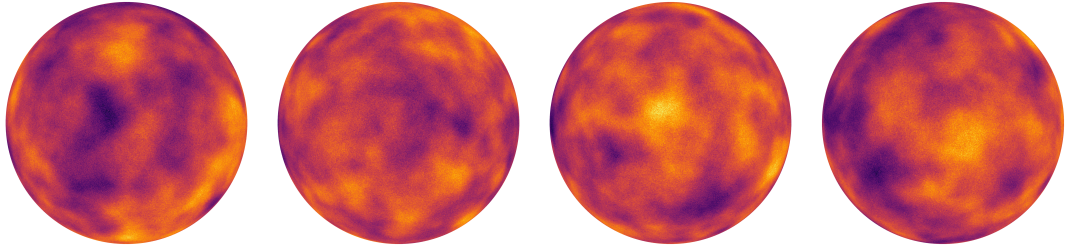


Figure 14: Different realizations of an isotropic Gaussian random field on \mathbb{S}^2 evaluated at a Fibonacci lattice with $N = 10^6$ points. All shown realizations assume values in the interval $[-4.1, 4.4]$. Darker colors correspond to smaller values.

In this example, we have $V_\ell = \mathcal{O}(2^{-\alpha\ell})$ as before, while the cost is now $C_\ell = \mathcal{O}(2^{2\ell})$, since the sphere is a two dimensional manifold and the n -d-tree becomes a quad-tree asymptotically. Therefore, we decrease the number of samples in this example by the factor $N_\ell/N_{\ell-1} = 2^{-(\alpha+2)/2} \approx 2^{-5/4}$. The convergence of the multilevel Monte Carlo approximation to the mean of the Gaussian process on \mathbb{S}^2 is shown in Figure 15. The figure shows the maximum error averaged over 10 runs. The error bars indicate one standard deviation. Over each of these runs, the Fibonacci lattice is kept fixed, while the interpolation points used for the multilevel Monte Carlo method are randomized in each leaf of the cluster tree. Nested interpolation points are again obtained by selecting the first non-empty child and assigning its sample point to the parent cluster. The theoretical rate of $N^{-1/2}$ is roughly achieved in this example.

9 Conclusion

We have developed a data-centric framework for the approximation of site-to-value maps. This framework covers both deterministic and empirical data sets in metric spaces. We have identified the discrete modulus of continuity as a natural and computable intrinsic regularity measure for discrete data. This makes the framework applicable to all site-to-value maps mapping from a compact metric space to a metric space. Our analysis shows the consistency of this regularity measure in the infinite data limit for deterministic and empirical data sites. Motivated by these findings, a data-intrinsic approximation theory for site-to-value maps has been introduced. For random site-to-value maps we have proposed multilevel approximation spaces and a variant of the multilevel Monte Carlo method to compute statistical quantities of interest. The obtained results

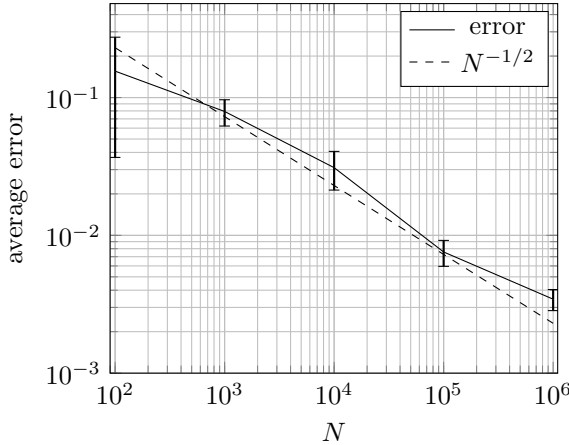


Figure 15: Average error of the multilevel Monte Carlo approximation of the mean of a Gaussian process on \mathbb{S}^2 for different N over 10 different runs. The error bars show one standard deviation.

can serve as a foundation for more intricate data-driven applications. In the numerical studies, synthetic and real-world data sets have been considered. The numerical results for the consistency of the discrete modulus of continuity and the validation of the discrete approximation error bounds corroborate the theoretical findings. The multilevel Monte-Carlo approximation of the expectation of a spatial low-regularity Gaussian random field on the sphere evaluated at a Fibonacci lattice clearly demonstrates the practical relevance of data-centric approaches.

Acknowledgements

JD received support from the DFG under Germany’s Excellence Strategy, project 390685813. MM was funded by the SNSF starting grant “Multiresolution methods for unstructured data” (TMSGI2_211684).

References

- [1] P. Assouad. Plongements lipschitziens dans \mathbb{R}^n . *Bulletin de la Société Mathématique de France*, 111(4):429–448, 1983.
- [2] S. Avesani, G. Giacchi, and M. Multerer. Multiresolution local smoothness detection in non-uniformly sampled multivariate signals. *arXiv preprint arXiv:2507.13480*, 2025.
- [3] A. Barth, C. Schwab, and N. Zollinger. Multi-level Monte Carlo finite element method for elliptic PDEs with stochastic coefficients. *Numerische Mathematik*, 119:123–161, 2011.
- [4] C. Bauckhage. ML2R coding nuggets greedy set cover with binary NumPy arrays. 2022.
- [5] Y. Benyamin and J. Lindenstrauss. *Geometric Nonlinear Functional Analysis*. Number 48. American Mathematical Society, Providence, 2000.
- [6] A. Beygelzimer, S. Kakade, and J. Langford. Cover trees for nearest neighbor. In *Proceedings of the 23rd International Conference on Machine Learning*, pages 97–104, 2006.
- [7] B. Bohn, J. Gärcke, and M. Griebel. *Algorithmic Mathematics in Machine Learning*. Society for Industrial and Applied Mathematics, Philadelphia, 2024.
- [8] L. Breiman. Random forests. *Machine Learning*, 45(1):5–32, 2001.
- [9] DWD Climate Data Center (CDC). 10-minute values of station observations of air temperature 2 m above ground in °C for germany, version v21,3. Accessed: 2025-09-11.

- [10] V. Chvátal. A greedy heuristic for the set-covering problem. *Mathematics of Operations Research*, 4(3):233–235, 1979.
- [11] K.L. Clarkson. Nearest-neighbor searching and metric space dimensions. In G. Shakhnarovich, T. Darrell, and P. Indyk, editors, *Nearest-Neighbor Methods in Learning and Vision: Theory and Practice*, pages 15–59, Cambridge, 2006. MIT Press.
- [12] R.R. Coifman and M. Maggioni. Diffusion wavelets. *Applied and Computational Harmonic Analysis*, 21(1):53–94, 2006.
- [13] T. H. Cormen, C. E. Leiserson, R. L. Rivest, and C. Stein. *Introduction to algorithms*. MIT Press, Cambridge, 2009.
- [14] C. de Boor. *A practical guide to splines*. Springer, New York, 2001.
- [15] R.A. DeVore and G.G. Lorentz. *Constructive Approximation*. Number 303. Springer, New York, 1993.
- [16] Z. Ditzian. Moduli of smoothness using discrete data. *Journal of Approximation Theory*, 49(2):115–129, 1987.
- [17] Z. Ditzian and A. Prymak. Discrete d -dimensional moduli of smoothness. *Proceedings of the American Mathematical Society*, 142(10):3553–3559, 2014.
- [18] Z. Ditzian and V. Totik. *Moduli of smoothness*. Springer, New York, 1987.
- [19] D.L. Donoho, M. Vetterli, R.A. DeVore, and I. Daubechies. Data Compression and Harmonic Analysis. *IEEE Transactions on Information Theory*, 44(6), 1998.
- [20] N. Dyn, E. Farkhi, and Mokhov A. *Approximation of Set-valued Functions*. Imperial College Press, London, 2014.
- [21] J. Dölz. Data sparse multilevel covariance estimation in optimal complexity. *arXiv preprint arXiv:2301.11992*, 2023.
- [22] G. Elefante, G. Giacchi, M. Multerer, and J. Quizi. Bespoke multiresolution analysis of graph signals. *arXiv preprint arXiv:2507.19181*, 2025.
- [23] G.B. Folland. *Real Analysis*. Wiley, New York, 1999.
- [24] M. Gavish, B. Nadler, and R.R. Coifman. Multiscale Wavelets on Trees, Graphs and High Dimensional Data: Theory and Applications to Semi Supervised Learning. In *ICML*, volume 10, pages 367–74, 2010.
- [25] M.B. Giles. Multilevel Monte Carlo methods. *Acta Numerica*, 24:259–328, 2015.
- [26] I. Goodfellow, Y. Bengio, and A. Courville. *Deep Learning*. Adaptive Computation and Machine Learning. The MIT press, Cambridge, Mass, 2016.
- [27] W. Hackbusch. *Hierarchical Matrices: Algorithms and Analysis*. Springer, Heidelberg, 2015.
- [28] H. Harbrecht, L. Herrmann, K. Kirchner, and C. Schwab. Multilevel approximation of Gaussian random fields: Covariance compression, estimation, and spatial prediction. *Advances in Computational Mathematics*, 50(5):101, 2024.
- [29] H. Harbrecht and M. Multerer. Samplers: Wavelet concepts for scattered data. In R. DeVore and A. Kunoth, editors, *Multiscale, Nonlinear and Adaptive Approximation II*, pages 299–326, Cham, 2024. Springer Nature.
- [30] H. Harbrecht, M. Multerer, O. Schenk, and C. Schwab. Multiresolution kernel matrix algebra. *Numerische Mathematik*, 156(3):1085–1114, 2024.
- [31] J. Heinonen. *Lectures on analysis on metric spaces*. Springer Science & Business Media, New York, 2001.

[32] J.S. Hesthaven and S. Ubbiali. Non-intrusive reduced order modeling of nonlinear problems using neural networks. *Journal of Computational Physics*, 363:55–78, June 2018.

[33] D. Jackson. *The Theory of Approximation*. American Mathematical Society, Providence, 1930.

[34] S. Jaffard. Pointwise smoothness, two-microlocalization and wavelet coefficients. *Publicacions Matemàtiques*, 35(1):155–168, 1991.

[35] S. Janson and S. Kaijser. *Higher moments of Banach space valued random variables*. American Mathematical Society, Providence, 2015.

[36] A.N. Kolmogorov and V.M. Tikhmirov. ε -entropy and ε -capacity of sets in functional spaces. In A. N. Shirayev and M. Hazewinkel, editors, *Selected Works of A. N. Kolmogorov*, pages 86–170, Dordrecht, 1993. Springer.

[37] B. Korte and J. Vygen. *Combinatorial Optimization: Theory and Algorithms*. Springer, Berlin, 2018.

[38] R. Krauthgamer and J.R. Lee. Navigating nets: Simple algorithms for proximity search. In *Proceedings of the Fifteenth Annual ACM-SIAM Symposium on Discrete Algorithms*, pages 798–807, 2004.

[39] H. Lebesgue. Sur les intégrales singulières. *Annales de la Faculté des Sciences de Toulouse*, 1:25–117, 1909.

[40] M. Ledoux and M. Talagrand. *Probability in Banach Spaces: isoperimetry and processes*. Springer, Berlin, 1991.

[41] L. Lu, P. Jin, G. Pang, Z. Zhang, and G. E. Karniadakis. Learning nonlinear operators via DeepONet based on the universal approximation theorem of operators. *Nature machine intelligence*, 3(3):218–229, 2021.

[42] S. Mallat. *A Wavelet Tour of Signal Processing*. Elsevier, San Diego, 1999.

[43] R. Marques, C. Bouville, M. Ribardiere, L. P. Santos, and K. Bouatouch. Spherical fibonacci point sets for illumination integrals. *Computer Graphics Forum*, 32(8):134–143, 2013.

[44] C.E. Rasmussen and C.K.I. Williams. *Gaussian processes for machine learning*. MIT Press, Cambridge, 2006.

[45] G. Santin, T. Wenzel, and B. Haasdonk. On the optimality of target-data-dependent kernel greedy interpolation in Sobolev reproducing kernel hilbert spaces. *SIAM Journal on Numerical Analysis*, 62(5):2249–2275, 2024.

[46] P. Slavík. A tight analysis of the greedy algorithm for set cover. In *Proceedings of the Twenty-Eighth Annual ACM Symposium on Theory of Computing*, Stoc ’96, pages 435–441, New York, 1996. Association for Computing Machinery.

[47] Statista. Big data, 2025. Accessed: 2025-09-01.

[48] K.-G. Steffens. *The History of Approximation Theory: From Euler to Bernstein*. Birkhäuser, Boston, 2006.

[49] V.V. Vazirani. *Approximation Algorithms*. Springer, Berlin, 2001.

[50] M. Vetterli. Wavelets, approximation, and compression. *IEEE Signal Processing Magazine*, 18(5):59–73, September 2001.

[51] H. Wendland. *Scattered data approximation*. Cambridge University Press, Cambridge, 2005.

[52] C.K.I. Williams and M. Seeger. Using the Nyström method to speed up kernel machines. In T.K. Leen, T.G. Dietterich, and V. Tresp, editors, *Advances in Neural Information Processing Systems 13 (NIPS 2000)*, pages 682–688, Cambridge, 2001. MIT Press.